Trabajo Fin de Máster

Máster en Física

Thermalization of an Isotropic Quantum Harmonic Oscillator

Autor: María del Pilar Morales Rodríguez

Tutores:

Luis Miguel Nieto Calzada

Blas Manuel Rodríguez Lara

Abstract

This work describes the most important states used in the field of quantum information: coherent states. We start with the definition of a Hamiltonian for a two-dimesional harmonic oscillator from which we construct the eigenstates called *Hermite-Gauss states* and *Laguerre-Gauss states*, which allow to describe the modes of a beam system. We continue describing the main coherent and thermal states that can be defined from the same Hamiltonian, this time they are visualized as eigenstates of the $SU(1,1)$ group generators and then for $SU(2)$. Subsequently, a theoretical system involving the input of a thermal state and an empty state in a beam splitter is discussed and experimentally compared.

Resumen

El presente trabajo cubre los estados más destacados que se utilizan en el ámbito de la información cuántica:los estados coherentes. Se inicia definiendo un hamiltoniano para un oscilador armónico bidimensional del cual se construyen los eigenestados llamados *estados de Hermite-Gauss* y *estados de Laguerre-Gauss*, los cuales permiten describir los modos de un sistema de haces. Continuamos describiendo los principales estados coherentes y termicos que se pueden definir a partir del mismo hamiltoniano, esta vez se visualizan como eigenestados de los generadores del grupo $SU(1,1)$ y luego para $SU(2)$. Posteriormente se aborda un sistema teórico que implica el ingreso de un estado térmico y un estado vacío en un divisor de haces el cual se logra comparar experimentalmente.

Contents

List of Figures

Chapter 1

Introduction

Quantum mechanics has taken a new approach in recent years, showing its potential to extend into domains traditionally governed by classical systems [1]. Quantum computation, quantum communication, and quantum information are some of the new areas of growing interest, where the former mainly seeks to overcome the limitations of classical computers by designing more efficient algorithms [2, 3], communication seeks to transmit qubits between remote locations, and quantum information perfects the speed of transmission and information processing [1, 2, 4]. These three areas are interrelated, and many of their advances, have been achieved through the application of quantum optics, given its focus on how to achieve control, manipulation and measurement of the properties of light [5, 6]. In this work, we will focus on examining one of the essential aspects of quantum optics and quantum information, specifically the quantum states from the perspective of the harmonic oscillator. This decision is due to the importance of the quantum harmonic oscillator in numerous areas, including quantum information processing [6–9].

The quantization of the electromagnetic field can be analogously analyzed as a many-particle system description [10]. Systems where there are well-defined numbers of photons for each mode of the field are described by the called Fock states or number states [11]. Since the quantization of the electromagnetic field in terms of ladder operators can be described as the Hamiltonian harmonic oscillator, Fock states can be obtained by repeated application of the creation operator on the ground state, which allow determines the energy [10–12]. While the Fock state possesses well-defined energy, it lacks a well-defined electric field; consequently, the expectation value of the field operator for a Fock state is zero [12]. Mathematically these are essentially eigenstates of the number operator, indicated its eigenvalue in number of photons excited in the calculated mode [11]. The interest in these states resides in the fact that they represent the fundamental states of the quantum theory of light and constitute a complete set of one-mode states that are easy to manipulate. However, it's important to note that their experimental implementation is not straightforward [12].

Moreover, one of the most extensively researched states is the coherent state [10]. Coherent states can be expressed as a superposition of Fock states [11], with the property that a coherent state can repeatedly absorb photons from an electromagnetic field without changing in any way [13, 14]. The coherent states, which are the closest equivalents to classical fields in the classical limit, were initially discovered by Schrödinger and constructed by Glauber while studying electromagnetic correlation functions [6, 15]. These states can be represented as eigenstates of the annihilation operators [11, 13]. The construction of coherent states can be achieved through two equivalent definitions [16, 17], one of which involves identifying them as eigenstates of the algebra's annihilation operator, called Barut-Girardello coherent state. The coherent states, defined by Gilmore-Perelomov coherent states, involve using a displacement operator on the system's empty state [14], in addition to coherent Perelomov states, squeezed states are obtained that correspond to states of minimum uncertainty [37, 38]. Coherent states are significant as a laser's output mimics them, and a single-mode laser that operates above its threshold

generates coherent state excitation suitable for experimental and theoretical analysis [10, 11].

When dealing with light sources that exhibit behavior in which a set of probabilities specifies the radiation field's range of states, the field's state becomes a mixed state. Mixed states are described using statistical distributions, a concept introduced in quantum mechanics through the density operator [11, 12].

One notable example of mixed states is thermal states. These states occur when examining a single-mode electromagnetic field in thermal equilibrium with cavity walls at temperature T [10, 12]. When radiation is weakly coupled to a thermal bath, the field can be treated as an isolated system, described statistically using the density operator [12, 18]. This scenario adheres to Planck's law, where the likelihood of n excited photons relies on a density operator based on number states. Number states serve as the appropriate basis for the density operator because the thermal distribution describes the system's probabilities in its energy eigenstates, which correspond to the number states [11].

Now, if we examine the transmission of light in optical systems defined as two-dimensional harmonic oscillators, two further crucial states can be incorporated into those described earlier. For beams that can be depicted in Cartesian coordinates, they display square symmetry, and it is best to use Hermite-Gauss states to examine them. In cases where beams exhibit ring symmetry, Laguerre-Gaussian states are utilized, allowing for the manipulation of the angular momentum of light.

This is particularly significant in classical and quantum communications as photons have the ability to carry orbital angular momenta (OAM). This property allows them to be used as data carriers in classical communications, and in quantum communications, they can be used to encode complementary information within a single photon [19, 19, 20, 20–24, 39]. Where the findings have been effectively used in interferometry, quantum communication, functional communication protocols, cryptography, imaging, and other areas [19, 20, 25–27].

However, as mentioned by Yao et al. in [20] and Shein et al. [25], the study of Gaussian beams, is a relatively new field that has gained popularity over time and although it is a powerful tool, the aforementioned states are still useful in the development of quantum computing, an example of this can be seen in [30] where he showed that interference of genuine multi-particle higher order Fock states is an effective approach in quantum simulations.

On the other hand, coherent states are valuable for exchanging information, establishing quantum key protocols, and other applications [31–33]. Another advantage of coherent states is their ability to generate entangled coherent states from their superposition [34], this generating an advantage for quantum computation over classical computation, since the first is capable of producing entangled qubits, like Browne indicate in [6], the counterpart to coherence in quantum optics is the quantum mechanical superposition of the qubit, being the qubits basic elements of quantum information technology [4, 34]. One way to produce entangled coherent state is through the use of a beam splitter [35], which consists of two inputs through which the states enter, and two outputs through which the new states are obtained. This device can be represented mathematically as an operator that transforms the system's states [11, 12, 36].However, the resulting state may or may not be an entangled state. For instance, if squeezed states are used as inputs, the degree of squeezing for the input fields will determine the entanglement of the output state of a beam splitter [36].

Besides entangling output optical fields, the beam splitter has multiple practical applications. It can be used to simulate processes such as quantum state loss, photon loss, and thermal environments [35, 36].

Furthermore, thermal states provide a comprehensive depiction of quantum systems and are utilized in a variety of circumstances such as quantum information processing, quantum teleportation, or quantum cryptography protocols [27, 32, 39]. For this case, when the density operator of the global system cannot be expressed as a weighted sum of tensor product states, we refer to it as a mixed entangled state. Entanglement can be viewed as a form of correlation

that permits more uncertainty in the states of local systems than in the state of the global system, which is unachievable in classical statistics [6]. For instance, only when a non-classical squeezed thermal state and vacuum enter the input port of a beam splitter, the output state will be entangled only if the squeezed thermal state is non-classical [36].

This work explores the generation of Hermite-Gaussian states and Laguerre-Gaussian states, enabling us to describe their associated modes. By incorporating the concept of orbital angular momentum, we gain insights into how the radial and azimuthal quantum numbers obtained can be linked to coherent states, which are here represented in two distinct formulations within the Lie algebra framework. Finally, we delve into the of mixed states, particularly in the context of thermal states. Explain in detail the scenario where a thermal state and a vacuum incident on the input port of a beam splitter, and establish correlations for the output states.

In Chapter 2, from the Hamiltonian of the isotropic harmonic oscillator two dimension, we first consider the linear momentum and the ladder operators, obtaining the so-called Hermite-Gauss states; subsequently, we consider the angular momentum and define new ladder operators, obtaining the Laguerre-Gauss states, which are related to the radial and azimuthal numbers. In Chapter 3 and 4 the coherent and mixed states are introduced, described as eigenstates of the generators of the group $SU(1,1)$ and $SU(2)$ respectively, considering the Fock space and angular momentum. In Chapter 5 the recognition of thermal states as the most well-known examples of mixed states is a pivotal starting point for us to explore, both theoretically and experimentally, the system where a thermal state and an empty state are entered independently to each of the inputs of a beam splitter. This gives a new thermal state described by the result obtained in both outputs. Finally, in Chapter 6 the results obtained are summarized and discussed.

Chapter 2

Two Dimensional Isotropic Harmonic Oscillator

The harmonic oscillator is quite useful to describe different physical events. For our work we will take advantage of the relation of its eigenstates with the Gaussian beams [40]. For this purpose, we'll start from the Hamiltonian of the harmonic oscillator in two dimensions, considering first the linear momentum, and then using orbital angular momentum, obtaining the Hermite-Gauss (HG) and Laguerre-Gauss (LG) states, respectively. These allow to describe the beams of a laser, thus receiving the name of Hermite-Gauss (HG) and Laguerre-Gauss (LG) modes in the field of the study of lasers. In the words of Nienhuis the Hermite-Gaussian modes resemble the factored eigenstates of the two-dimensional quantum harmonic oscillator [41].

We begin by considering the Hamiltonian of a particle of mass m, moving in a two-dimensional harmonic potential with frequency ω that depends on two coordinates, where ξ_1 and ξ_2 are the position operators for the fist and second coordinate respectively. Similar for the momentum operators $\hat{\eta}_j$, $j = 1, 2$, we'll have the following Hamiltonian, it is an isotropic harmonic oscillator [42],

$$\hat{H} = \frac{1}{2} \sum_{j=1,2} \left(\frac{\hat{\eta}_j^2}{m} + m\omega^2 \hat{\xi}_j^2 \right). \tag{2.1}$$

By making a correct change of variables, we can write the Hamiltonian in dimensionless canonical coordinates and in differential form, see Table 2.1.

Original Variables	Dimensionless canonical variables	Position space	Moment space
$\hat{\xi}_j$	$\hat{q}_j = \sqrt{\frac{m\omega}{\hbar}}\,\hat{\xi}_j$	$\hat{\xi}_j = \xi_j$ $\hat{p}_j = p_j$	$\hat{\xi}_j = i\hbar\frac{\partial}{\partial \eta_j}$ $\hat{q}_j = i\frac{\partial}{\partial p_j}$
$\hat{\eta}_j$	$\hat{p}_j = \frac{1}{\sqrt{\hbar m\omega}}\hat{\eta}_j$	$\hat{\eta}_j = -i\hbar\frac{\partial}{\partial \xi_j}$ $\hat{p}_j = -i\frac{\partial}{\partial q_j}$	$\hat{\eta}_j = \eta_j$ $\hat{p}_j = p_j$

Table 2.1: Re-normalized dimensionless canonical variables, where $j = 1, 2$, represents the corresponding coordinate.

Hence,

$$\hat{H} = \frac{\hbar\omega}{2} \sum_{j=1,2} \left(q_j^2 - \frac{\partial^2}{\partial q_j^2} \right), \tag{2.2}$$

It is possible to simplify this Hamiltonian by the use of ladder operators, which are defined as,

$$\hat{a}_j = \frac{1}{\sqrt{2}} \left(q_j + \frac{\partial}{\partial q_j} \right), \qquad \hat{a}_j^\dagger = \frac{1}{\sqrt{2}} \left(q_j - \frac{\partial}{\partial q_j} \right), \quad j = 1, 2. \tag{2.3}$$

For convenience, we will use the differential form of the ladder operators instead of the canonical variable operators, which satisfy the following commutation relations:

$$\left[\hat{a}_k, \hat{a}_l^\dagger \right] = \delta_{kl}, \quad \left[\hat{H}_k, \hat{a}_l \right] = -\hbar\omega \hat{a}_k \, \delta_{kl}, \quad \left[\hat{H}_k, \hat{a}_l^\dagger \right] = \hbar\omega \hat{a}_k^\dagger \, \delta_{kl}, \quad k, l = 1, 2. \tag{2.4}$$

The Hamiltonian $\hat{H}$ can be expresed in terms of the anticonmmutador as,

$$\hat{H} = \hbar\omega \frac{1}{2} \sum_{j=x,y} \left\{ \hat{a}_j^\dagger, \hat{a}_j \right\}, \tag{2.5}$$

and the number operator is $\hat{N}_j = \hat{a}_j^\dagger \hat{a}_j$, $j = 1, 2$.

2.1 Eigenvalues

Since the Hamiltonian commutes with every number operator, $\hat{H}$ and $\sum_{j=1,2} \hat{N}_j$ can have a set of joint eigenstates [42], which will be denoted by $|n_1; n_2\rangle$, where $|n_1; n_2\rangle = |n_1\rangle \otimes |n_2\rangle$,

The number operator acts on the states as:

$$\hat{N}_1 \, |n_1; n_2\rangle = n_1 \, |n_1; n_2\rangle \tag{2.6}$$

$$\hat{N}_2 \, |n_1; n_2\rangle = n_2 \, |n_1; n_2\rangle \tag{2.7}$$

Applying $\hat{H}$ (defined in eq.(2.5)) to the previous state $|n_1, n_2\rangle$

$$\hat{H} \, |n_1; n_2\rangle = E_{n_1;n_2} \, |n_1; n_2\rangle \tag{2.8}$$

it is easy see,

$$E_{n_1;n_2} = \hbar\omega \, (n_1 + n_2 + 1) \, . \tag{2.9}$$

Normalizing the states we have that,

$$\hat{a}_j \, |n_j\rangle = \sqrt{n_j} \, |n_j - 1\rangle \tag{2.10}$$

$$\hat{a}_j^\dagger \, |n_j\rangle = \sqrt{n_j + 1} \, |n_j + 1\rangle \tag{2.11}$$

this implies that when $\hat{a}$ operate on $|n_j\rangle$, it decrease n by one unit. Since there is no negative energy, the lowest state known as the ground state is established.

$$|0; 0\rangle = |n_1 = 0, \, n_2 = 0\rangle \, . \tag{2.12}$$

In the case of $\hat{a}^\dagger$, it increase n by one unit so, the state $|n_1; n_2\rangle$ can be obtained by the successive application the operators $\hat{a}_1^\dagger \, \hat{a}_2^\dagger$, such that

$$|n_1; n_2\rangle = \frac{1}{\sqrt{n_1! \, n_2!}} \left(\hat{a}_1^\dagger \right)^{n_1} \left(\hat{a}_2^\dagger \right)^{n_2} |0; 0\rangle \, . \tag{2.13}$$

with $n_j = 0, 1, 2, \ldots$ and $j = 1, 2$. with $n_j = 0, 1, 2, \ldots$ and $j = 1, 2$. In the case of the beam study, n_1 and n_2 denote the (transverse) mode numbers. So this can be understood as the creation of excitation in the transversal modes starting from the vacuum state $|0; 0\rangle$, [40, 41] .

2.2 Hermite-Gauss states

As we know that energy cannot be extracted beyond the lowest state, it is possible to know the form of that state, on which the rest of the states will be built, for this we start from the fact that,

$$\langle q|n_1;n_2\rangle = \psi_{n_1;n_2}(q_1,q_2), \tag{2.14}$$

$$\psi_{n_1;n_2}(q_1,q_2) = \psi_{n_1}(q_1)\psi_{n_2}(q_2), \tag{2.15}$$

Therefore, it is sufficient to study only one state $\psi_{n_j}(q_j)$ to know the 2D harmonic oscillator's eigenstates. So for this part we will omit the subscript j, since we know beforehand that we only use the one-dimensional ladder operators and it can belong to any of the possible spaces. Using eq.(2.10) we can write the equation $\hat{a}_j\,|n_j=0\rangle$ in the position space, as

$$\langle q|\,\hat{a}\,|0\rangle = \frac{1}{\sqrt{2}}\left(q+\frac{\partial}{\partial q}\right)\psi_0(q) = 0,$$

So we get the differential equation

$$q\psi_0(q) + \psi_0'(q) = 0 \tag{2.16}$$

Solve and Normalizing

$$\psi_0(q) = \left(\frac{1}{\pi}\right)^{1/4}\exp\left(-\frac{1}{2}q^2\right), \tag{2.17}$$

Which corresponds to a Gaussian function, [43].
The first excited state corresponds to applying the operator $\hat{a}^\dagger$ on the ground state, $\psi_1(q) = \langle q|\,\hat{a}^\dagger\,|0\rangle$. So for the nth excited state

$$\langle q|n\rangle = \langle q|\,\frac{\left(\hat{a}^\dagger\right)^n}{\sqrt{n!}}\,|0\rangle = \frac{1}{\sqrt{n!}}\frac{1}{\sqrt[n]{2}}\left(q-\frac{d}{dq}\right)^n\psi_0(q). \tag{2.18}$$

We can rewrite the above as,

$$\psi_n(q) = \frac{1}{\sqrt[4]{\pi}}\frac{1}{\sqrt{2^n n!}}\left(q-\frac{d}{dq}\right)^n\exp\left\{\left(-\frac{q^2}{2}\right)\right\}. \tag{2.19}$$

Wave functions and the Hermite polynomials

If we consider the next identity operator [42],

$$\exp\left\{\left(-\frac{q^2}{2}\right)\right\}\left(q-\frac{d}{dq}\right)\exp\left\{\left(\frac{q^2}{2}\right)\right\} = -\frac{d}{dq}. \tag{2.20}$$

Applying the operator n times,

$$\exp\left\{\left(-\frac{q^2}{2}\right)\right\}\left(x-\frac{d}{dq}\right)^n\exp\left\{\left(\frac{q^2}{2}\right)\right\} = (-1)^n\frac{d^n}{dq^n}. \tag{2.21}$$

Applying on the left-hand side $\exp\left\{\left(\frac{q^2}{2}\right)\right\}$ and on the right-hand side $\exp\{(-q^2)\}$,

$$\left(q-\frac{d}{dq}\right)^n\exp\left\{\left(-\frac{q^2}{2}\right)\right\} = (-1)^n\exp\left\{\left(\frac{q^2}{2}\right)\right\}\frac{d^n}{dq^n}\exp\{(-q^2)\}. \tag{2.22}$$

but

$$(-1)^n\exp\left\{\left(\frac{q^2}{2}\right)\right\}\frac{d^n}{dq^n}\exp\{(-q^2)\} \;=\; \exp\left\{\left(-\frac{q^2}{2}\right)\right\}H_n(y),$$

where $H_n(q)$ are the **Hermite polynomials**,

$$H_n(q) = \left[(-1)^n \mathrm{e}^{q^2} \frac{d^n}{d(q)^n} \mathrm{e}^{-q^2}\right], \tag{2.23}$$

and,

$$\left(q - \frac{d}{dq}\right)^n \exp\left\{\left(-\frac{q^2}{2}\right)\right\} = \exp\left\{\left(-\frac{q^2}{2}\right)\right\} H_n(q). \tag{2.24}$$

So the states ψ_n, defined in eq.(2.19), can be written in terms of the Hermite polynomials,

$$\psi_n(q) = \frac{1}{\sqrt[4]{\pi}} \frac{1}{\sqrt{2^n n!}} \exp\left\{\left(-\frac{q^2}{2}\right)\right\} H_n(q), \tag{2.25}$$

the functions $\psi_{2n}(q)$ are even (i.e. $\psi_{2n}(-q) = \psi_{2n}$) and $\psi_{2n+1(q)}$ are odd (i.e., $\psi_{2n+1}(-q) = -\psi_{2n+1}(q)$) so, the Hermite polynomials H_{2n} are even and H_{2n+1} are odd. The meaning of this is the wave functions of even one-dimensional potentials have definite parity [42].

So back to our two dimensional problem that the state eq.(2.15), can be written in terms of Hermite polynomials,

$$\psi_{n_1;n_2}(q_1, q_2) = \frac{1}{\sqrt{\pi 2^{n_1+n_2} n_1! n_2!}} \exp\left\{\left(-\frac{q_1^2 + q_2^2}{2}\right)\right\} H_{n_1}(q_1) H_{n_2}(q_2), \tag{2.26}$$

Figure 2.1 shows the intensity distribution, $|\psi_{n_1,n_2}(q_1, q_2)|^2$, for some Hermite-Gauss modes in dimensionless canonical phase space, (q_1, q_2), for transversal excitation numbers $n_1; n_2 = 0, 1, 2, 3$. For highe-oders modes we can note that if the value of n_1 remains invariant, the increase of n_2 will be seen as an upward separation of the mode and otherwise if the n_2 axis remains invariant, the mode will extend in space to the right. The mean value of the transversal excitation numbers is associate with the number of modes in the corresponding direction [44,45]. Solutions of in terms of Hermite polynomials aren't unique, it's possible to construct alternate

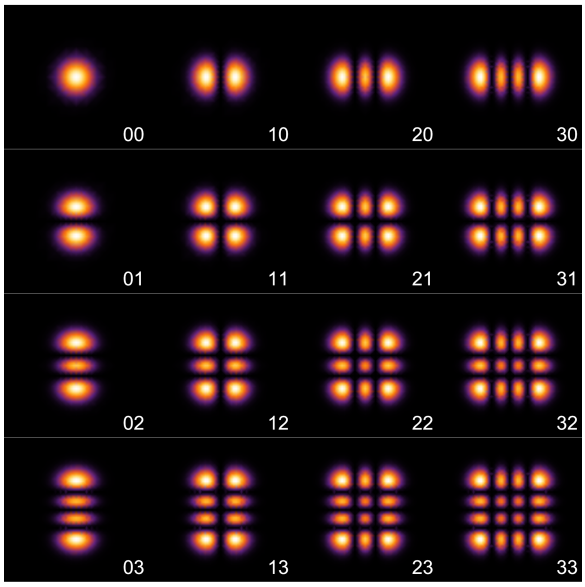

Figure 2.1: Intensity distribution for Hermite-Gauss modes, $|\psi_{n_1,n_2}(q_1, q_2)|^2$. The first number corresponds to n_1 and the second to n_2, so the mode shown in $n_1 = 0$, $n_2 = 0$ is the fundamental mode. High-order modes, had a distribution most spread out radially than the fundamental mode.

solutions due to the isotropic dimensionless Hamiltonian of the harmonic oscillator, guarantee the invariance of any of the axes compared to infinitesimal rotations generated by the angular momentum operator, which will be conserved [13]. So in the next section we'll focus in obtain circular quanta operators.

2.3 Angular momentum

To describe the system more broadly it is sometimes necessary to expand the problem about its behavior on other physical elements that it affects, in this case the angular momentum.

Let's start by considering the $\hat{L}_3$ component of angular momentum defined as

$$\hat{L}_3 = \hat{q}_1\hat{p}_2 - \hat{q}_2\hat{p}_1 = i\hbar\left(\hat{a}_1\hat{a}_2^\dagger - \hat{a}_1^\dagger\hat{a}_2\right). \tag{2.27}$$

Using the Hamiltonian seen in eq.(2.5), it is easy see $\left[\hat{H}, \hat{L}_3\right] = 0$, this proves that both operators have a basis of eigenvectors in common. So it is possible to write new operators as a combination of the ladder operators $\hat{a}_1, \hat{a}_2$ $(\hat{a}_1^\dagger, \hat{a}_2^\dagger)$, where these operators will act as azimutal operators.

2.3.1 Right and left circular quanta

We define new ladder operators, defined as,

$$\hat{a}_\pm = \frac{1}{\sqrt{2}}\left(\hat{a}_1 \mp i\hat{a}_2\right), \qquad \hat{a}_\pm^\dagger = \frac{1}{\sqrt{2}}\left(\hat{a}_1^\dagger \pm i\hat{a}_2^\dagger\right). \tag{2.28}$$

The operators $\hat{a}_\pm$ are commonly referred to as destruction operators *right (−) and left (+) "circular quanta",*, where $\hat{a}_\pm^\dagger$ the corresponding creation operators [43]. Knowing the action of the $\hat{a}_j$, $j = 1, 2$ operators and their respective adjoints operators for a state $|\psi_{n_1;n_2}\rangle$. It is expected the action of the operators $\hat{a}_\pm$ on a state $|\psi_{n_1;n_2}\rangle$, generates a combination of state $|\psi_{n_1-1,n_2}\rangle$, with $|\psi_{n_1;n_2-1}\rangle$.

Thus $\hat{a}_\pm$ and $\hat{a}_\pm^\dagger$ are analogous to the ladder operators $\hat{a}_j$, $\hat{a}_j^\dagger$, $j = 1, 2$. Being similar in their commutation properties.

$$\left[\hat{a}_+, \hat{a}_+^\dagger\right] = \left[\hat{a}_-, \hat{a}_-^\dagger\right] = 1. \tag{2.29}$$

2.3.2 Eigenvectors

To obtain the eigenvectors of the harmonic oscillator in this new base, consider the raising operators $\hat{a}_+^\dagger$, $\hat{a}_-^\dagger$ on the state $|0;0\rangle$, which will generate a new state, denoted by $|n_+;n_-\rangle$, such that

$$|n_+;n_-\rangle = \frac{1}{\sqrt{(n_+)!\,(n_-)!}}\left(\hat{a}_+^\dagger\right)^{n_+}\left(\hat{a}_-^\dagger\right)^{n_-}|n_1 = 0; n_2 = 0\rangle. \tag{2.30}$$

Because of the way ladder operators are defined, the state $|n_+;n_-\rangle$, will be a composition of the states generated by $|n_1 = 0; n_2 = 0\rangle$. More generally, since we have two options, $n_+ > n_-$ and $n_- > n_+$. If consider $(\hat{a}_+^\dagger)^{n_+}(\hat{a}_+^\dagger)^{-n_+} = I$, eq.(2.30), could rewrite,

$$|n_+;n_-\rangle = \frac{1}{\sqrt{(n_+)!\,(n_-)!}}\begin{cases}\left(\hat{a}_+^\dagger\hat{a}_-^\dagger\right)^{n_-}\left(\hat{a}_+^\dagger\right)^{(n_+-n_-)}|n_1 = 0; n_2 = 0\rangle, & n_+ > n_- \\ \left(\hat{a}_+^\dagger\hat{a}_-^\dagger\right)^{n_+}\left(\hat{a}_-^\dagger\right)^{(n_--n_+)}|n_1 = 0; n_2 = 0\rangle, & n_- > n_+\end{cases} \tag{2.31}$$

2.3.3 Eigenvalues

We are now interested in how n_+ and n_- are related to the eigenvalues of the angular momentum operator and those of the harmonic oscillator Hamiltonian, so it is convenient to define new numbers operators,

$$\hat{N}_+ = \hat{a}_+^\dagger\hat{a}_+ = \frac{1}{2}\left(\hat{a}_1^\dagger\hat{a}_1 + \hat{a}_2^\dagger\hat{a}_2 - i\hat{a}_1^\dagger\hat{a}_2 + i\hat{a}_1\hat{a}_2^\dagger\right), \tag{2.32a}$$

$$\hat{N}_- = \hat{a}_-^\dagger\hat{a}_- = \frac{1}{2}\left(\hat{a}_1^\dagger\hat{a}_1 + \hat{a}_2^\dagger\hat{a}_2 + i\hat{a}_1^\dagger\hat{a}_2 - i\hat{a}_1\hat{a}_2^\dagger\right) \tag{2.32b}$$

The eq.(2.5) and eq.(2.27) can be written as,

$$\hat{L}_3 = \hbar \left(\hat{N}_+ - \hat{N}_- \right), \tag{2.33}$$

$$\hat{H} = \hbar\omega \left(\hat{N}_+ + \hat{N}_- + 1 \right). \tag{2.34}$$

Respectively.

Operating $\hat{L}_3$ and $\hat{H}$ on $|n_+; n_-\rangle$,

$$\hat{L}_3 \, |n_+; n_-\rangle = \hbar(n_+ - n_-) \, |n_+; n_-\rangle \,, \tag{2.35a}$$
$$\hat{H} \, |n_+; n_-\rangle = \hbar\omega(n_+ + n_- + 1) \, |n_+; n_-\rangle \,. \tag{2.35b}$$

Where the eigenvalue of $\hat{H}$ is similar to that found in the previous section (eq.(2.9)). For the case of eigenvalues of $\hat{L}_3$, it is convenient to definite,

$$\ell = n_+ - n_-, \tag{2.36}$$

to get

$$\hat{L}_3 \, |n_+; n_-\rangle = \hbar \, \ell \, |n_+; n_-\rangle \,. \tag{2.37}$$

Here we note that $\hat{a}_+^\dagger$ increases the angular momentum by a factor $\hbar$,

$$\hat{L}_3 \, \hat{a}_+^\dagger \, |n_+; n_-\rangle = \hbar \, [(n_+ + 1) - n_-)] \, |n_+ + 1; n_-\rangle \,, \tag{2.38}$$

Doing the same for $\hat{a}_-^\dagger$ we find that the angular momentum increases by a factor $-\hbar$

With this we have, as expected, that the values of $\ell = 0, \pm 1, \pm 2, \pm 3, \ldots$. However, it should not be forgotten that H and L have the same base in common, therefore it is convenient to see how the values $n_\pm$ are, with respect to the system, we can do $n = n_+ + n_-$, resulting in

$$\hat{H} \, |n_+; n_-\rangle = \hbar\omega(n + 1) \, |n_+; n_-\rangle \,, \tag{2.39}$$

Since the values of $n_\pm$ must satisfy the form of the eigenvalues of $\hat{H}$, we have

$$\left\langle \hat{N}_+ + \hat{N}_- \right\rangle = n_+ + n_- = n, \tag{2.40}$$

where n can be any positive integer, but composed of any possible combination of n_+ and n_-, that is, n_+ could be zero and n_- could be n, or perhaps $n_+ = n - 2$ while $n_- = 2$. The only condition is that $n_\pm$ be positive integers or zero and their sum results in a number n.

For the case of $\hat{L}_3$, for an energy level $(n+1)\hbar\omega$ and knowing that $\ell = n_+ - n_-$, the possible values of l are

$$\ell = n \,, n - 2 \,, n - 4, \ldots, -n + 2, -n. \tag{2.41}$$

A way of to relate the possible values of l and the values of $n_\pm$ can be given from its construction,

$$\begin{array}{cc} \text{If} & \text{So} \\ \left\langle \hat{a}_+^\dagger \hat{a}_+ \right\rangle = n_+ = j; & \left\langle \hat{a}_-^\dagger \hat{a}_- \right\rangle = n_- = n - j, \end{array} \tag{2.42}$$

with $j = 0, 1, \ldots, n$. Being the angular component

$$\left\langle \hat{L}_3 \right\rangle = \hbar \, (n_+ - n_-) = \hbar \, (n - 2j) \,, \tag{2.43}$$

Likewise the states $|n_+ = n; n_- = 0\rangle$, $|n_+ = 0; n_- = n\rangle$, correspond to the maximum and minimum value for $\hat{L}_3$, which are visualized as the vectors of circular polarization (circular movements to the right or to the left) of the classical field associated with a given value of the total energy [43]

Since circular motions are described, it is convenient to change our system to polar coordinates.

2.4 Laguerre-Gauss states

It is convenient to study the harmonic oscillator operators defined in eq.(2.28) in polar coordinates:

$$q_1 = r\cos(\phi), \qquad r \geq 0, \tag{2.44}$$
$$q_2 = r\sin(\phi), \qquad 0 \leq \phi < 2\pi, \tag{2.45}$$

it implies that,

$$\psi_{n_1,\,n_2}(q_1,q_2) \longrightarrow \psi_{n_1;n_2}(r,\phi) = \frac{\mathrm{e}^{-\frac{r^2}{2}} H_{n_1}\left(r\cos(\phi)\right) H_{n_2}\left(r\sin(\phi)\right)}{\sqrt{\pi}\sqrt{n_1!n_2!2^{n_1+n_2}}}, \tag{2.46}$$

and if we choose

$$\langle q(r,\phi)|n_+;n_-\rangle = \chi_{n_+,n_-}(r,\phi), \tag{2.47}$$

we have a new set of states, which are related to angular momentum [41, 46]

$$\chi_{n_+,n_-}(r,\phi) = \frac{(-1)^{n_-}n_-!}{\sqrt{\pi}\sqrt{n_-!(\ell+n_-)!}}\, r^{\ell}\exp\left(-\frac{1}{2}\,(r)^2\right) L^{\ell}_{n_-}\left(r^2\right)\mathrm{e}^{(i\ell\phi)} \tag{2.48}$$

Here $L^{\ell}_{n_-}$ is the **generalized Laguerre polynomial** of order n_- and degree ℓ, where $\ell = n_+ - n_-$ and $\ell = n\,, n-2\,, n-4, \ldots, -n+2, -n$, with n the excited level. These states have the form of the Laguerre–Gaussian modes [47], and allow to study the structure of the system which consists of p dark concentric rings for a given azimuthal number ℓ [46].

If we define the azimuthal mode index ℓ and the radial mode index p [9],

$$\begin{aligned} p &= n_-, \\ \ell &= n_+ - n_-, \end{aligned} \tag{2.49}$$

we may rewrite eq.(2.31) as

$$|p;\,\ell\rangle = \frac{1}{\sqrt{(p)!\,(p+|\ell|)!}}\left(\hat{a}^{\dagger}_{+}\hat{a}^{\dagger}_{-}\right)^{p}\begin{cases}\left(\hat{a}^{\dagger}_{+}\right)^{|\ell|}|0;0\rangle\,, & \ell>0,\\ \left(\hat{a}^{\dagger}_{-}\right)^{|\ell|}|0;0\rangle\,, & \ell<0.\end{cases} \tag{2.50}$$

by projecting over the complete basis $|r;\phi\rangle$ we get the corresponding wave function $\psi_{p,\ell}(r,\phi)$ in the transverse (dimensionless) parameters.

$$\begin{aligned} \psi_{p,\ell}(r,\phi) &= \langle r;\phi|p;\,\ell\rangle\,, \\ &= \frac{1}{\sqrt{\pi}}(-1)^{p}\sqrt{\frac{p!}{(p+|\ell|)!}}\, r^{|\ell|}\mathrm{e}^{-\frac{1}{2}r^2}\mathrm{L}^{|\ell|}_{p}(r^2)\mathrm{e}^{i\ell\phi}, \end{aligned} \tag{2.51}$$

in terms of the associated Laguerre polynomials $\mathrm{L}^{|\ell|}_{p}(\rho^2)$ [46].

Figure 2.2 shows the intensity distribution, $|\psi_{p,\ell}(r,\phi)|^2$, for some Laguerre-Gauss modes, for radial and azimuthal numbers $p, \ell = 0, 1, 2, 3$. For highe-oders modes we can note that for $p = 0$, (first column) with $\ell = 1, 2, 3$ exists only a single-ring mode called *doughnut modes*, for $p = 1$ and $\ell = 1, 2, 3$ we observe two rings so in general for $\ell \neq 0$, the intensity pattern of LG beams had $p + 1$ concentric rings, if $\ell = 0$ there are p rings around the center Gaussian mode, then ℓ determines its size [23, 48].

Now operating $\hat{L}_3$ and $\hat{H}$ on $|p;\,\ell\rangle$,

$$\hat{L}_3\,|p;\,\ell\rangle = \hbar\,\ell\,|p;\,\ell\rangle\,, \tag{2.52a}$$
$$\hat{H}\,|p;\,\ell\rangle = \hbar\omega(2p+\ell+1)\,|p;\,\ell\rangle\,, \tag{2.52b}$$

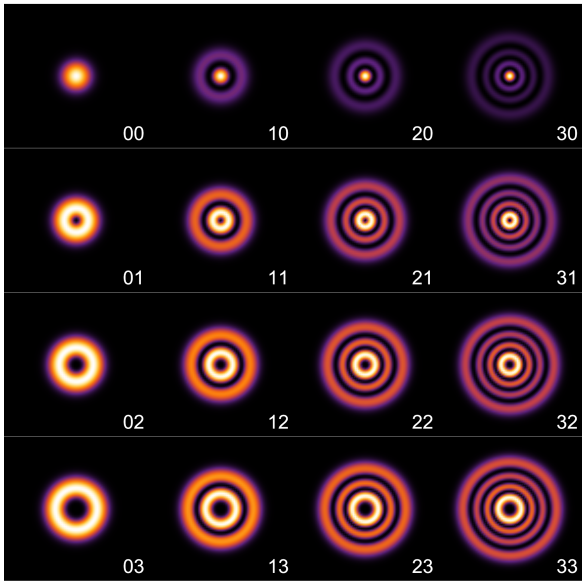

Figure 2.2: Intensity distribution for Laguerre-Gauss modes, $|\psi_{p,\ell}(r,\phi)|^2$. The first number corresponds to the radial number p and the second to the azimuthal number ℓ, so the mode shown in $p = 0$, $\ell = 0$ is a Gaussian mode.

from $\hat{H}$ we obtain the relation

$$n = n_1 + n_2 = 2p + |\ell|, \tag{2.53}$$

the absolute value in ℓ indicate that n is always a positive number. Some authors work with the so-called radial number operator $\langle\hat{p}\rangle = p = 0, 1, 2, \ldots$ [9, 46]. Both representations, with the same Hilbert space bases ($\mathcal{H} = \mathcal{H}_1 \times \mathcal{H}_2$, spanned by the eigenstates $|n_1; n_2\rangle$,) are in essence equivalent and equally valid due to there is no structurally determined symmetry in free space. So in rectangular coordinates the mode fields are described by a set of Hermite-Gaussian functions resulting in Hermite-Gaussian modes being appropriate for treat problems with square symmetry, whereas in polar coordinates they are described by Laguerre-Gaussian functions, so the Laguerre-Gauss modes are appropriate to treat problems with axial symmetry [44, 45, 49]. In quantum physics and even more in quantum optics there are two families of states that are of great interest, the pure states, which are those that are completely coherent and the mixed states that are a superposition of the coherent states, both analyzed theoretical and experimental [50]. So far, we have approached the eigenstates of the harmonic oscillator from the perspective of the creation and destruction operators and their representation in the linear or polarized basis, however, using the harmonic oscillator we can study the coherent states, which are the most classical of the states of the oscillator, these means constitutes a state of minimum uncertainty. However, coherent states may be constructed for an angular momentum system with some differences of the oscillator coherent states [51]. And consider that the Laguerre-Gauss states cover the whole Hilbert space, where the transverse momentum and the orbital angular momentum are conserved. This Hilbert space can be partitioned and each partition can be represented in terms of the Lie group generators $SU(1,1)$ and $SU(2)$ [51, 52], different representations of the system can be studied in coherent and mixed states.

Chapter 3

States Associated with the Group $SU(1,1)$

The circular quanta right and left creation and annihilation operators given in (2.28) allow the construction of a dimensionless representation of the algebra $su(1,\,1)$

$$\hat{K}_+ = \hat{a}_+^\dagger \hat{a}_-^\dagger, \qquad \hat{K}_- = \hat{a}_+ \hat{a}_-, \qquad \hat{K}_0 = \frac{1}{2}\left(\hat{a}_+^\dagger \hat{a}_+ + \hat{a}_-^\dagger \hat{a}_- + 1\right), \tag{3.1}$$

where $\hat{K}_0$, $\hat{K}_+$ y $\hat{K}_-$ are the generators of this algebra, being $\hat{K}_\pm$ ladder operators, and

$$\hat{K}^2 = \frac{1}{4}\left[\left(\hat{a}_+^\dagger \hat{a}_+ - \hat{a}_-^\dagger \hat{a}_-\right)^2 - 1\right] \tag{3.2}$$

the Casimir operator. They satisfy the commutation relations,

$$\left[\hat{K}_+, \hat{K}_-\right] = -2\hat{K}_0, \qquad \left[\hat{K}_0, \hat{K}_\pm\right] = \pm\hat{K}_\pm, \qquad \left[\hat{K}^2, \hat{K}_j\right] = 0. \tag{3.3}$$

The corresponding group $SU(1,1)$ is the simplest non-abelian (i.e. non-commutative) group, so the Lie algebra corresponding to this group considers different representations of irreducible, discrete, continuous and supplementary unitary series. However, the discrete representations of this algebra are used for the description of physical systems [37, 38, 53], where the standard orthonormal basis for this representation is

$$\hat{K}_+ \left|k; m\right\rangle = \sqrt{(2k+m)(m+1)}\left|k; m+1\right\rangle, \tag{3.4}$$
$$\hat{K}_- \left|k; m\right\rangle = \sqrt{(2k+m-1)m}\left|k; m-1\right\rangle, \tag{3.5}$$
$$\hat{K}_0 \left|k; m\right\rangle = (k+m)\left|k; m\right\rangle, \tag{3.6}$$
$$\hat{K}^2 \left|k; m\right\rangle = k\,(k-1)\left|k; m\right\rangle, \tag{3.7}$$

where $k > 0$ is the so-called Bargmann parameter. Knowing this, we can now study some different representations generated by this Lie algebra.

3.1 Radial representation

Using the standard representation (3.4)–(3.7) $\left|k; m\right\rangle = k\,(k-1)\left|k; m\right\rangle$, to obtain the eigenvalue of the Casimir operator, and applying $\hat{K}^2 = \frac{1}{4}\left((\hat{N}_+ - \hat{N}_-)^2 - 1\right)$ to the state $\left|n_+; n_-\right\rangle$, we get

$$\hat{K}^2 \left|n_+; n_-\right\rangle = \frac{1}{4}\left[(n_+ - n_-)^2 - 1\right]\left|n_+; n_-\right\rangle = \frac{1}{4}\left[\ell^2 - 1\right]\left|n_+; n_-\right\rangle, \tag{3.8}$$

Comparing (3.7) and (3.8), we have $k^2 - k - \frac{1}{4}\left[\ell^2 + 1\right] = 0$, and it is easy to get

$$k = \frac{1}{2}(|\ell| + 1). \tag{3.9}$$

Similarly, for the rest of the operators. It's convenient to define new states in terms of p and k given in (2.49), such that

$$|n_+; n_-\rangle \to |k; p\rangle\,. \tag{3.10}$$

Then

$$\hat{K}^2\,|k;p\rangle = k\,(k-1)\,|k;p\rangle\,, \tag{3.11}$$
$$\hat{K}_0\,|k;p\rangle = (k+p)\,|k;p\rangle\,, \tag{3.12}$$
$$\hat{K}_+\,|k;p\rangle = \sqrt{(2k+p)(p+1)}\,|k;p+1\rangle\,, \tag{3.13}$$
$$\hat{K}_-\,|k;p\rangle = \sqrt{(2k+p-1)p}\,|k;p-1\rangle\,. \tag{3.14}$$

The raising and lowering operators $\hat{K}_\pm$ acting on a Laguerre-Gauss mode $|p,\ell\rangle$ increase or decrease the radial number p, however don't change the value of ℓ, this implies that, they conserve the Bargmann parameter for any value of p, with $p \geq 0$, [9, 46].

The Bargmann parameter $k = (|\ell| + 1)/2 = 1/2, 1, 3/2$ depends only on the azimuthal number operator, implies there will be two subspaces labeled with the same Bargmann parameter, one for each sign of the mean value of the azimuthal number except for zero. This allows us to define a relation between the Bargmann subspace basis and the Laguerre-Gauss states:

$$\langle r;\phi|k;p\rangle \equiv \langle r,\phi||\ell| = 2k-1;\, p\rangle = \psi_{2k-1,\,p}(r,\phi), \tag{3.15}$$

with $\langle r;\phi|k;p\rangle$ defined in eq(2.51).
The ladder operators $\hat{K}_\pm$ acting on $|k;p\rangle$ increase or decrease the radial number p. Thus, each infinite dimensional Bargmann subspace consists of states with equal azimuthal excitation number and progressive radial excitation number.

If now the group generators are used to define a unitary operator, acting on the lowest state $|k; m = 0\rangle$, we obtain the Gilmore-Peremolov coherent states.

3.2 Gilmore-Perelomov coherent states

The Gilmore-Perelomov coherent states for the $su(1,1)$ algebra are defined [37],

$$|k;\zeta\rangle = \mathrm{e}^{\xi\hat{K}_+ - \xi^*\hat{K}_-}|k;0\rangle = (1-|\zeta|^2)^k \mathrm{e}^{\xi\hat{K}_+}|k;0\rangle = (1-|\zeta|^2)^k \sum_{p=0}^{\infty}\sqrt{\frac{\Gamma(p+2k)}{p!\;\Gamma(2k)}}\zeta^p\;|k;p\rangle, \tag{3.16}$$

where $\xi = \frac{1}{2}\theta\mathrm{e}^{-i\omega}$, $\zeta = (\frac{\xi}{|\xi|})\tanh|\xi| = -\tanh\!\left(\frac{1}{2}\theta\right)\mathrm{e}^{-i\omega}$. With $\omega \in [0, 2\pi)$, $-\infty < \theta < \infty$, and the parameter ζ is restricted by $|\zeta| < 1$, this condition shows that these states are defined in the interior of a unit disk [37, 38]. Being the states $|k;\zeta\rangle$ normalized but not orthogonal:

$$\langle k;\zeta_1|k;\zeta_2\rangle = (1-|\zeta_1|^2)^k(1-|\zeta_2|^2)^k(1-|\zeta_1^*\zeta_2|^2)^{-2k}. \tag{3.17}$$

In dimensionless canonical space,

$$\langle r;\phi|k;\zeta\rangle = (1-|\zeta|^2)^k \sum_{p=0}^{\infty}\sqrt{\frac{\Gamma(p+2k)}{p!\Gamma(2k)}}\zeta^p\,\langle r;\phi|k;p\rangle\,, \tag{3.18}$$

$$= \frac{\left(1-|\zeta|^2\right)^k}{\sqrt{\pi(2k-1)!}} r^{2k-1}\mathrm{e}^{-\frac{1}{2}r^2}\mathrm{e}^{i\ell\phi}\sum_{p=0}^{\infty}(-\zeta)^p \mathrm{L}_p^{2k-1}\left(r^2\right), \tag{3.19}$$

where we have used the identity

$$(1-\alpha)^{m+1}\sum_{n=0}^{\infty}\alpha^n L_n^m(x)=\exp\left\{\frac{\alpha}{\alpha-1}\,x\right\} \tag{3.20}$$

and make $\psi_{k;\zeta}=\langle r,\phi|k;\zeta\rangle$, where

$$\psi_{k,\zeta}=\begin{cases}\mathcal{A}_{k,\theta}\,\mathrm{e}^{i(2k-1)\phi}, & \ell>0,\\ \mathcal{A}_{k,\theta}, & \ell=0,\\ \mathcal{A}_{k,\theta}\,\mathrm{e}^{-i(2k-1)\phi}, & \ell<0,\end{cases} \tag{3.21}$$

being

$$\mathcal{A}_{k,\theta}=\left[\frac{1+\tanh\left(\frac{\theta}{2}\right)}{1-\tanh\left(\frac{\theta}{2}\right)}\right]^{k} r^{2k-1}\sqrt{\frac{1}{\pi(2k-1)}}\exp\left\{-\frac{1}{2}\left(\frac{1+\tanh\left(\frac{\theta}{2}\right)}{1-\tanh\left(\frac{\theta}{2}\right)}\right)r^2\right\}. \tag{3.22}$$

These states are also eigenstates of the OAM, and present the same characteristics as those introduced in [46]. However, we present their analysis in terms of the Bargmann parameter, given the relation $|\ell|=2k-1$, so they are shape invariant in the time evolution. The average number of sharp rings in the state $\psi_{k,\xi}$ is

$$\overline{p}=2k\frac{|\zeta|^2}{|\zeta|^2-1}. \tag{3.23}$$

Figure 3.1 shows the probability of distribution and probability for (3.21). We can highlight that the densities are equivalent to the intensity distribution for Laguerre-Gauss modes with $p=0,\ell$ (see Figure 2.2). This is due to the fact that it is a coherent state that maintains the value of p but varies ℓ by varying the Bargamm's parameter given its relationship (3.9).

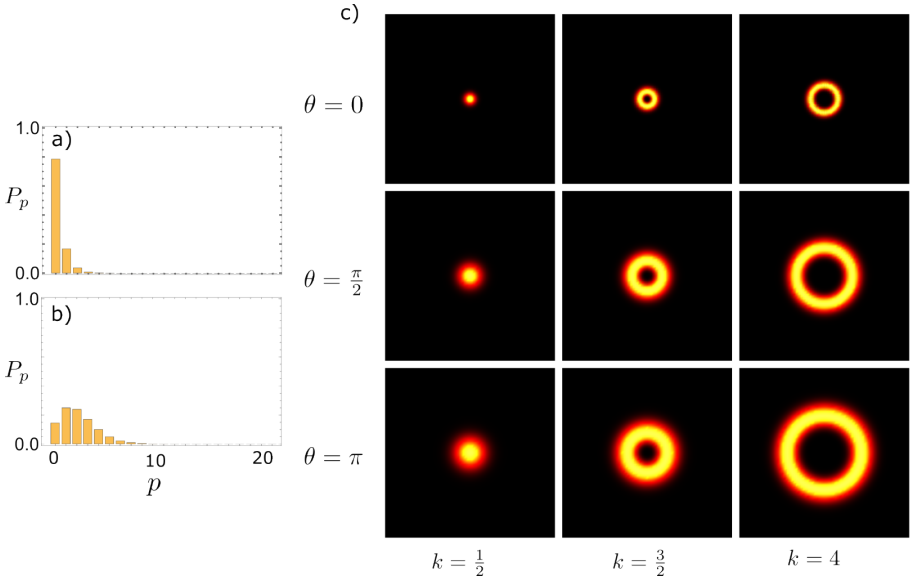

Figure 3.1: Probability distribution in the constant azimuthal number basis $\{|k;m\rangle\}$ for a Gilmore-Perelomov coherent states $|k;\zeta\rangle$ for Bargmann parameter a) $k=\frac{1}{2}$ and b) $k=4$. In c) the probability density function, $|\langle r,\phi|k;\zeta\rangle|^2$, of the wave function in dimensionless configuration space for different coherent phase values $\theta=0,\pi/2,\pi$, for Bargmann parameter $k=\frac{1}{2},\frac{3}{2},4$.

On the other hand, in Figure 3.2 we show the phase distribution of (3.21). Here we can emphasize that the number of vortices is directly proportional to the value of ℓ, in similar way there exists a rotation that depends of the θ value, which will be cyclic in a period of π.

Other states in the $su(1,1)$ representation are the coherent states of Barut and Girardelo, which are constructed as eigenstates of ladder operators representing discrete series [54], as we will show in the following section.

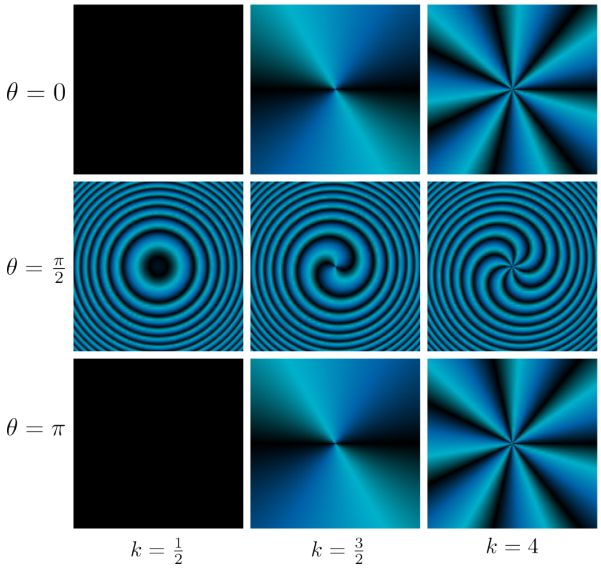

Figure 3.2: Phase distribution for a Gilmore-Perelomov coherent states, $\arg(\langle r, \phi | k; \zeta, \theta \rangle)$, in dimensionless configuration space for different coherent phase values $\theta = 0, \pi/2, \pi$, for Bargmann parameter $k = \frac{1}{2}, \frac{3}{2}, 4$.

3.3 Barut-Girardello coherent states

The Barut-Girardello coherent states for the $su(1,1)$ algebra, [37, 54], are such that

$$\hat{K}_- |k; z\rangle = z |k; z\rangle, \tag{3.24}$$

with $z \in \mathbb{C}$ and k the Bargmann parametrer. The expansion of these states on an orthonormal basis is,

$$|k; z\rangle = \frac{z^{k-1/2}}{\sqrt{I_{2k-1}(2\,|z|)}} \sum_{n=0}^{\infty} \frac{z^n}{\sqrt{n!\Gamma(2k+n)}} \, |k; z\rangle \,, \tag{3.25}$$

with $\mathrm{I}_\nu(x)$, a modified Bessel function of the first kind of ν–order:

$$I_\nu(z) = \sum_{n=0}^{\infty} \frac{\left(\frac{1}{2}z\right)^{\nu+2n}}{n!\Gamma(\nu+n+1)}. \tag{3.26}$$

The Barut-Girardello coherent states are normalized but not orthogonal [37].

For real negative coherent parameter, $z < 0$, the Barut-Girardello coherent state is given by

$$\langle r, \phi | k; z\rangle = \frac{(-1)^{-k+1/2} \mathrm{e}^{-z}}{\sqrt{\pi \, \mathrm{I}_{2k-1}(2|z|)}} \, \mathrm{e}^{-\frac{1}{2}r^2} \mathrm{J}_{2k-1}\left(2\sqrt{-z}\, r\right) \mathrm{e}^{i(2k-1)\phi}, \tag{3.27}$$

and therefore takes a Bessel function form in dimensionless canonical space.

Figure 3.3 shows the probability distribution and probability density for eq.(3.27), similar to the Gilmore-Peremolov states presented previously. The density is equivalent to the intensity distribution for Laguerre-Gauss modes, see (2.2), with $p = 0, \ell$, but in reverse.

Figure 3.4 shows the phase distribution of (3.27), where anew the number of vortices is directly proportional to the value of ℓ. However, remarkable differences are shown at $\theta = \pi$, the process being cyclic with a period of 2π.

Coherent states are highly efficient as they represent the most classical states attainable. Nevertheless, in laboratory settings, mixed states are often created. These states cannot be characterized by state vectors, but instead by a density operator [12]. Given their nature, these are usually found as thermal states, and given their importance for this work, we will analyze their representation in the group basis $SU(1,1)$.

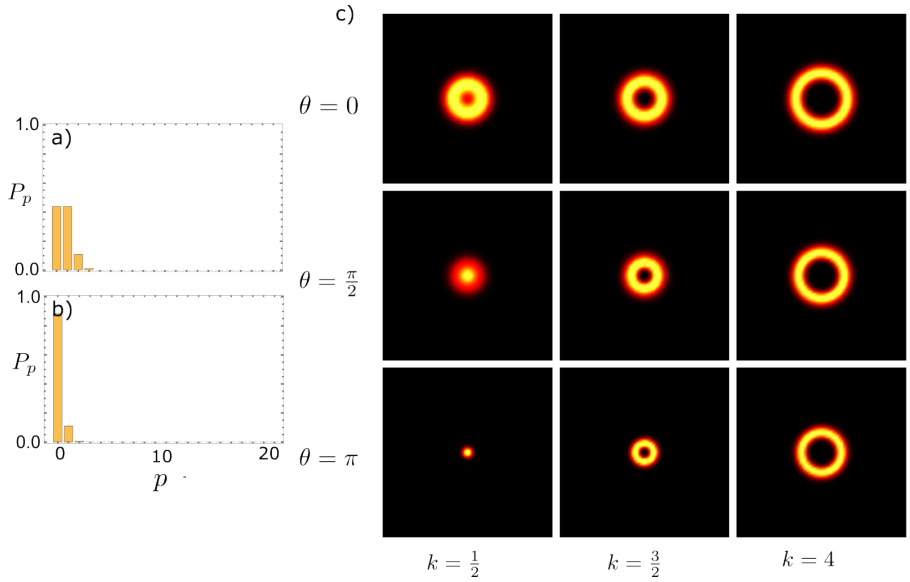

Figure 3.3: Probability distribution in the constant azimuthal number basis, $\{|k;m\rangle\}$ for a Barut-Girardello coherent states, $|k;z\rangle$ for Bargmann parameter a) $k = 1/2$ and b) $k = 4$. In c) probability density function, $|\langle r,\phi|k;z\rangle|^2$, of the wave function in dimensionless configuration space for different coherent phase values $\theta = 0, \pi/2, \pi$, for Bargmann parameter $k = 1/2, 3/2, 4$.

3.4 Thermal states

We now considered the thermal state $\rho_{\rm th}$, with β the Boltzmann's constant, T the temperature of the system, and $\hat{H}$ the Hamiltonian [11, 12],

$$\rho_{\rm th} = \frac{\mathrm{e}^{-\beta\hat{H}}}{\mathrm{Tr}\left(\mathrm{e}^{-\beta\hat{H}}\right)}, \qquad \beta = \frac{1}{k_B T}, \tag{3.28}$$

For our case, we take the Hamiltonian related to the harmonic oscillator eq.(2.34) in terms of the $su(1,1)$ algebra operators,

$$\hat{H} = 2\hbar\omega\hat{K}_0, \tag{3.29}$$

and has a diagonal form,

$$\hat{H} = 2\hbar\omega\left[\sum_{u=1}^{\infty}\sum_{v=0}^{\infty}\left(\frac{u}{2}+v\right)\left|\frac{u}{2};v\right\rangle\left\langle\frac{u}{2};v\right|_{+} + \sum_{u=2}^{\infty}\sum_{v=0}^{\infty}\left(\frac{u}{2}+|v|\right)\left|\frac{u}{2};v\right\rangle\left\langle\frac{u}{2};v\right|_{-}\right], \tag{3.30}$$

in the basis $|k;p\rangle_{\pm}$, with $k = u/2$ and $v = p$, and where we use the positive subscript to refer to zero and positive azimuthal numbers, $\ell \geq 0$, and the negative subscripts to negative azimuthal numbers, $\ell < 0$.

Thus, the thermal state in this basis is

$$\begin{aligned}\rho_{th} &= \frac{\left(\mathrm{e}^{\hbar\omega\beta}-1\right)^2}{\mathrm{e}^{\hbar\omega\beta}}\left\{\sum_{u=1}^{\infty}\sum_{v=0}^{\infty}\mathrm{e}^{-\hbar\omega(u+2v)\beta}\left|\frac{u}{2};v\right\rangle\left\langle\frac{u}{2};v\right|_{+} + +\sum_{u=2}^{\infty}\sum_{v=0}^{\infty}\mathrm{e}^{-\hbar\omega(u+2v)\beta}\left|\frac{u}{2};v\right\rangle\left\langle\frac{u}{2};v\right|_{-}\right\} \\ &= \frac{1}{\overline{n}(\overline{n}+1)}\left\{\sum_{u=1}^{\infty}\sum_{v=0}^{\infty}\left[\frac{\overline{n}}{(\overline{n}+1)}\right]^{u+2v}\left|\frac{u}{2};v\right\rangle\left\langle\frac{u}{2};v\right|_{+} + +\sum_{u=2}^{\infty}\sum_{v=0}^{\infty}\mathrm{e}^{-\hbar\omega(u+2v)\beta}\left|\frac{u}{2};v\right\rangle\left\langle\frac{u}{2};v\right|_{-}\right\}\end{aligned}$$

in terms of the Boltzmann parameter β or the average excitation number [12]

$$\mathrm{e}^{-\hbar\omega\beta} = \frac{\overline{n}}{\overline{n}+1}. \tag{3.31}$$

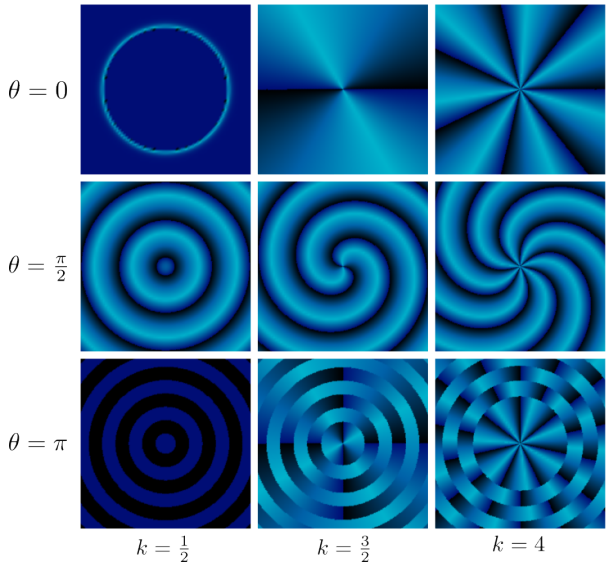

Figure 3.4: Phase distribution for a Barut-Girardello coherent states, $\arg(\langle r, \phi | k; z, \theta \rangle)$, in dimensionless configuration space for different coherent phase values $\theta = 0, \pi/2, \pi$, for Bargmann parameter $k = 1/2, 3/2, 4$.

Unlike the traditional representation of coherent states in the Fock basis, here we have developed coherent states based on radial and azimuthal numbers. We established the relationship between these numbers and transverse numbers in the previous section (see eq.(2.49)). Both the Gilmore-Perelomov and Barut-Girardello coherent states, exhibit radial information in their probability density, indicating that the coherence is characterized by the preservation of the number of rings. In the same way as in the Laguerre-Gauss states, the azimuthal number $|\ell|$ establishes the width of the ring, although the coherent state parameter θ can also modify the width of the ring. The differences between the Gilmore-Peremolov coherent states and the Barut-Girardello coherent states become apparent when examining their phase structures. While both exhibit vortices defined by the azimuthal number linked to the Bargmann parameter (eq.(3.9)), their periods differ, and the coherent states of Barut-Girardello also feature ring rotations at $\theta = \pi$.

If we now consider the superposition of the states, it is possible to obtain them as thermal states eq.(3.28). If we consider the two possible values of the azimuthal number $\pm\ell$ the density operator will be established as the sum of the density operators for each system. However, the thermal states associated with the group $SU(1,1)$ are not optimal for examining a system with a relatively small number of photons, because although the average value of these can be handled, their shape here described , associated to the group $SU(1,1)$, is established in an infinite Hilbert space [38], where this characteristic can be observed in the fact that the value of the azimuthal number $\ell \in \pm\infty$. For this reason, when looking for a finite Hilbert space that allows minimizing the work, we will consider the group $SU(2)$ in the next chapter.

Chapter 4

States Associated with the Group $SU(2)$

In a similar way as we obtained the states in the representation of $SU(1,1)$, we obtain those for the Lie algebra $su(2)$, which is spanned by the generators J_+, J_- and J_0, satisfying the commutation relations,

$$\left[\hat{J}_+, \hat{J}_-\right] = 2\hat{J}_0, \qquad \left[\hat{J}_0, \hat{J}_\pm\right] = \pm\hat{J}_\pm, \qquad \left[\hat{J}^2, \hat{J}_j\right] = 0, \quad j = 1, 2, \tag{4.1}$$

where the ladder operators can be rewritten as $\hat{J}_\pm = \hat{J}_1 \pm i\hat{J}_2$. In the Jordan-Schwinger representation of the $su(2)$ algebra [56] in terms of our circular polarization operators[1], we have

$$\hat{J}_+ = \hat{a}_+^\dagger \hat{a}_-, \qquad \hat{J}_- = \hat{a}_+ \hat{a}_-^\dagger, \qquad \hat{J}_0 = \frac{1}{2}\left(\hat{a}_+^\dagger \hat{a}_+ - \hat{a}_-^\dagger \hat{a}_-\right), \qquad \hat{J}^2 = \frac{1}{4}\hat{N}\left(\hat{N} + 2\right), \tag{4.2}$$

with $\hat{N} = \hat{N}_+ + \hat{N}_-$, previously defined (2.32). Similarly as we did in the study of group generators $su(1,1)$, for $su(2)$, by applying the operators described in eq.(4.2), to a state , we can obtain its corresponding eigenvalues, where in general form,

$$\begin{aligned}
\hat{J}_+ |j;m\rangle &= \sqrt{(j-m)(j+m+1)}\, |j;m+1\rangle\,, \\
\hat{J}_- |j;m\rangle &= \sqrt{(j+m)(j-m+1)}\, |j;m-1\rangle\,, \\
\hat{J}_0 |j;m\rangle &= m\, |j;m\rangle\,, \\
\hat{J}^2 |j;m\rangle &= j(j+1)\, |j;m\rangle\,,
\end{aligned} \tag{4.3}$$

4.1 Radial representation

In a similar way to what was done in the previous chapter, applying the operators defined in (4.2) to the state $|n_+, n_-\rangle$, and comparing with (4.3), we find that for its radial representation it is enough to write j and m as:

$$j = \frac{n_+ + n_-}{2} = \frac{n}{2} = \frac{2p + |\ell|}{2}, \qquad m = \frac{n_+ - n_-}{2} = \frac{\ell}{2}, \tag{4.4}$$

where the eq.(4.3), establishes that the lowest and the highest state to which the rising and lowering operators can be applied are

$$\hat{J}_\pm |j;\pm j\rangle_J = 0 \tag{4.5}$$

[1] It's possible to describe it also in terms of the ladder operators of the Cartesian canonical variables.

so $j = 0, 1/2, 1, 3/2, 2, \ldots$ and $j \geq m \geq -j$. The parameter j implies there will be two subspaces label with the same value, one for each sign of the mean value of the azimuthal number except for zero. This allows us to define

$$\langle r;\phi|j;m\rangle \equiv \langle r,\phi|p = j - |m|;\, |\ell = 2m\rangle = \psi_{j-|m|,2m}(r,\phi), \tag{4.6}$$

so the ladder operators $\hat{J}_\pm$ acting on $|j,m\rangle$ increase or decrease the azimuthal number $\ell/2$. Thus, each subspace consists of states with equal radial excitation number and progressive azimuthal excitation number. To construct the coherent states in this representation an operator must be defined in terms of the ladder operators $SU(2)$, from the previous section, we can deduce that these will be the Gilmore-Perelomov coherent states.

4.2 Gilmore-Perelomov coherent states

The Gilmore-Perelomov coherent states for the $su(2)$ algebra are defined [57, 58],

$$\begin{aligned} |j;\xi\rangle &= \mathrm{e}^{\left(\xi\hat{J}_+ - \xi^*\hat{J}_-\right)}|j;0\rangle = (1+|\tau|^2)^{-j}\mathrm{e}^{\tau\hat{J}_+}|j;0\rangle \\ &= \left(1+|\tau|^2\right)^{-j}\sum_{m=-j}^{j}\sqrt{\frac{(2j)!}{(j+m)!(j-m)!}}\tau^{j+m}\,|j;m\rangle\,, \end{aligned} \tag{4.7}$$

where $\xi = \frac{1}{2}\theta\mathrm{e}^{-i\omega}$, $\tau = \tan\left(\frac{1}{2}\theta\right)\mathrm{e}^{-i\omega}$, $0 \leq \theta \leq \pi$, $0 \leq \omega \leq 2\pi$. As in the previous representation, the CS-GPs are not orthogonal:

$$\langle j;\xi_1|j;\xi_2\rangle = \frac{(1+\tau_1^*\,\tau_1)^{2j}}{\left(1+|\tau_1|\right)^2\left(1+|\tau_2|\right)^2}. \tag{4.8}$$

If we want to write this result in terms of ℓ and p, we will see that it becomes more complex compared to the previous section, this is because the term j is written in terms of both, so we must be very careful when making the change in the sum. This case will not be discussed here. However, it is possible to obtain the $SU(2)$ Perelomov coherent states, for the harmonic oscillator in two dimensions in terms of j and m, in a similar way as it was obtained for $SU(1,1)$,

$$\langle r;\phi|j;\xi\rangle = \left(1+|\tau|^2\right)^{-j}\sum_{m=-j}^{j}\sqrt{\frac{(2j)!}{(j+m)!(j-m)!}}\tau^{j+m}\,\langle r;\phi|j;m\rangle \tag{4.9}$$

$$= \frac{\left(1+|\tau|^2\right)^{-j}}{\sqrt{\pi}}\mathrm{e}^{-\frac{1}{2}r^2}\sum_{m=-j}^{j}\frac{\sqrt{(2j)!}}{(j+m)!}(\tau)^{j+m}(-1)^{j-|m|}r^{2|m|}\mathrm{L}_{j-|m|}^{2|m|}\left(r^2\right)\,\mathrm{e}^{2im\phi}. \tag{4.10}$$

This result is similar to the one found in [59], for the standard $SU(2)$ Perelomov coherent states for two-dimensional harmonic oscillator. However, here we provide a brief analysis of their relationship with the states of Laguerre-Gauss and Hermite-Gauss.

In Figure 4.1 we show the probability distribution and the probability density for eq.(4.10), we can note that the density is very similar to the intensity distribution for the Hermite-Gaussian modes, being a result of interest that emphasizes the relationship that exists with the quantum numbers p and ℓ and the numbers n_1 and n_2 of the modes.

In Figure 4.2 we show the phase distribution of (4.10). We can notice that the phase structures shift occurs in a more abrupt way compared to the plots shown in the previous section. The number of variations in the distribution or in the phase structure is directly proportional to $2j+1$. Similar results have been found in recent studies on the structure of light [60, 61].

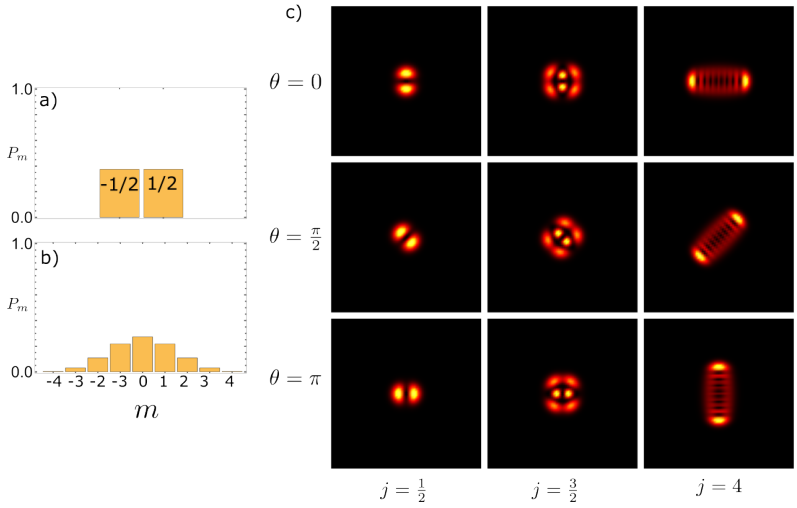

Figure 4.1: Probability distribution in the constant excitation basis, $\{|j;m\rangle\}$, for Gilmore-Perelomov coherent states, $|j;\xi\rangle$, for the parameter (a) $j = 1/2$ and (b) $j = 4$. In c) probability density function, $\arg(\langle r,\phi|j;\xi,\theta\rangle)$, in dimensionless configuration space for different coherent phase values $\theta = 0, \pi/2, \pi$ for $j = 1/2, 3/2, 4$.

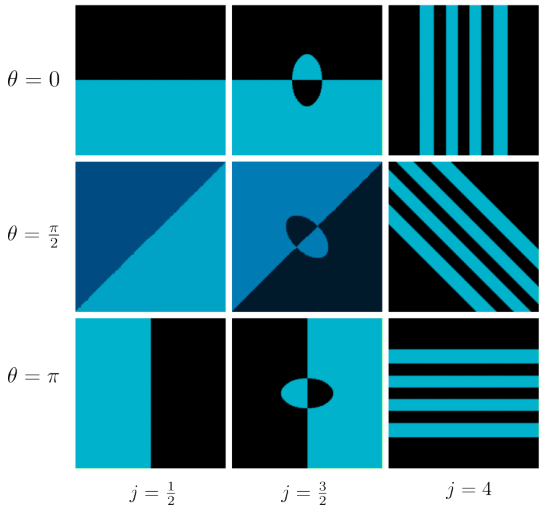

Figure 4.2: Phase distribution for a Gilmore-Perelomov coherent states, $\arg(\langle r,\phi|j;\xi,\theta\rangle)$, in dimensionless configuration space for different coherent phase values $\theta = 0, \pi/2, \pi$, for $j = 1/2, 3/2, 4$.

4.3 Barut-Girardello coherent states

For the Barut-Girardello coherent states, there is no representation, because $\hat{J}_-|j;m\rangle = \xi|k;z\rangle$, but for the lowest state $\hat{J}_-|j;-j\rangle = 0$.

4.4 Thermal states

Similar to how the thermal state was constructed in the previous section, we can write its representation for $su(2)$, by first writing the Hamiltonian (2.34) such that,

$$\hat{H} = \hbar\omega(\hat{J}_N + 1), \tag{4.11}$$

where we defined a total number operator, $\hat{J}_N|j;m\rangle = 2j|j;m\rangle$, and has a diagonal form,

$$\hat{H} = \hbar\omega \sum_{u=0}^{\infty} \sum_{v=-u/2}^{u/2} (u+1) \left|\frac{u}{2};v\right\rangle \left\langle\frac{u}{2};v\right|, \tag{4.12}$$

in the basis $|j;m\rangle$, with $u = 2j = n_+ + n_-$ and $v = 2m = n_+ - n_-$. Thus, the thermal state in this basis is

$$\hat{\rho}_{th} = \left(1 - \mathrm{e}^{-\hbar\omega\beta}\right) \sum_{u=0}^{\infty} \sum_{v=-u/2}^{u/2} \mathrm{e}^{-\hbar\omega u\beta} \left|\frac{u}{2};v\right\rangle \left\langle\frac{u}{2};v\right| = \sum_{u=0}^{\infty} \frac{\overline{n}^u}{(\overline{n}+1)^{u+1}} \sum_{v=-u/2}^{u/2} \left|\frac{u}{2};v\right\rangle \left\langle\frac{u}{2};v\right|, \tag{4.13}$$

where the first equality is written in terms of the Boltzmann parameter and the second one is in terms of the average excitation number (3.31).

Choosing which of the representations we have discussed is the best will depend on the system to be analyzed. Thus, coherent states can be adapted from the study of the interaction of matter with an electric field [62], studies of optical media [63], to their application in quantum information [31], as well as in quantum communication.

Much information about coherent states can be found in the literature. Currently the panorama is being expanded by making use of thermal states [32], for example they have been used with the intention of generating a distribution of quantum keys (secret key generator) with a view to generating wireless quantum communication. Therefore, in the next chapter we will focus on the study of thermal states.

Chapter 5

An Experiment with Thermal States

Thermal states have had a recent boom in their possible applications. Among other things, they have been used to generate Ghost images, which involves generating two images of an object through two detectors, where one will not see the object and the other will. None of the detectors will form an image by itself, but can be reconstructed. The effect can be achieved with reduced visibility by means of correlated thermal light, thus mimicking it in the classical environment [64]. At the same time, this allows the development of ideas about teleportation which consists of translate any quantum state from one place to another, without physically moving it [27]. In general we find that it is important to obtain a beam correlation, which is achieved by separating the light derived from a thermal source, this is possible if it is incident on a beam splitter (BS), which will separate the light in two different paths [11, 12].

5.1 Beam Splitter

The beam splitter consist in two input and two output arms of beams, for a classical beam splitter with a classical light field of complex amplitude E_1 incident on one of the inputs, there will be two output beams E_2 and E_3. As pointed out in [12], if R and T are the (complex) reflectance and transmittance respectively of the beam splitter, then

$$E_2 = R\,E_1 \qquad E_3 = TE_1. \tag{5.1}$$

For the quantum beam splitter, if both cases were compatible for any number of photons we could replace classical complex field amplitudes E_i by a set of annihilation operators $\hat{a}_i$. But given the commutation relations, we find that

$$\hat{a}_2 = R\hat{a}_1 + T'\hat{a}_0, \qquad \hat{a}_3 = T\hat{a}_1 + R'\hat{a}_0, \tag{5.2}$$

where $\hat{a}_0$ represents the field operator of the classically vacant input mode. R' and T' indicated the existence of two sets of transmittances and reflectances, allowing for the possibility of an asymmetric beam splitter. So if we only have one input beam, the other input will have a vacuum state, where fluctuations will continue to affect the system [12]. The input and output modes are related according to

$$\hat{a}_2 = \frac{\hat{a}_0 + i\,\hat{a}_1}{\sqrt{2}}, \qquad \hat{a}_3 = \frac{i\,\hat{a}_0 + \hat{a}_1}{\sqrt{2}}. \tag{5.3}$$

Thus, the beam splitter can be represented by a unitary transformation, defined by

$$\hat{U}_{bs}(\zeta) = \exp\Big[\zeta\hat{a}_0^\dagger\hat{a}_1 - \zeta^*\hat{a}_1^\dagger\hat{a}_0\Big], \tag{5.4}$$

where $\zeta = \theta\,\mathrm{e}^{-i\phi}$, with $\theta, \phi \in \mathbb{R}$, being θ an amplitude and ϕ the phase difference between the reflected and transmitted fields [36]. The quantum and classical treatments of beam splitters

agree for coherent and thermal beams ("classical"-like light beams), but with a single or few photons, the classical approach to beam splitting produces erroneous results [12]. Here we will focus on the thermal states affecting a quantum beam splitter. But here we can ask ourselves what we call the thermal state, which is what we will describe in the next section.

5.2 Thermal states

A thermal state is a description of a thermal light, this means, a light beam emitted by a thermal sourse (a source in thermal equilibrium) can be described by a density matrix [12, 32],

$$\hat{\rho} = \sum_i p_i \left|\psi_i\right\rangle \left\langle\psi_i\right|, \tag{5.5}$$

where ψ_i are the states vectors, and p_i is the probability of the system being in the ith state of the ensamble $|\psi_i\rangle$, considering the temperature T of a system described by its Hamiltonian $\hat{H}$, the thermal state can be written

$$\hat{\rho}_{\text{th}} = \frac{\mathrm{e}^{-\beta\hat{H}}}{\text{Tr}\left(\mathrm{e}^{-\beta\hat{H}}\right)}, \tag{5.6}$$

with $\beta = 1/(k_B T)$ the Boltzmann's constant and Tr the trace:

$$\text{Tr}\left(e^{-\beta\hat{H}}\right) = \sum_{n=0}^{\infty} e^{-E_n\beta}. \tag{5.7}$$

From (5.5) and (5.6), is easy to deduce that

$$p_i = \left\langle\psi_i\right| \hat{\rho} \left|\psi_i\right\rangle = \frac{\mathrm{e}^{-\beta E_i}}{\sum_i \mathrm{e}^{-\beta E_i}}, \tag{5.8}$$

more in particulary, here p_i in the probability that the mode is thermally excited in the i-th level [12]. If we now consider a two-dimensional isotropic harmonic oscillator in thermal equilibrium, we have,

$$e^{-\beta\hat{H}} = \sum_{n_1;n_2=0}^{\infty} e^{-\hbar\omega(n_1+n_2+1)\beta} \left|n_1;n_2\right\rangle \left\langle n_1;n_2\right|, \tag{5.9}$$

and

$$\text{Tr}\left(e^{-\beta\hat{H}}\right) = e^{\hbar\omega\beta}\left(e^{\hbar\omega\beta}-1\right)^{-2}. \tag{5.10}$$

Hence, finally we have

$$\hat{\rho}_{th} = \left(1-e^{-\hbar\omega\beta}\right)^2 \sum_{n_1;n_2=0}^{\infty} e^{-\hbar\omega(n_1+n_2)\beta} \left|n_1;n_2\right\rangle \left\langle n_1;n_2\right|. \tag{5.11}$$

If we consider the average number of photons, then

$$\overline{n} = \frac{1}{\mathrm{e}^{-\hbar\omega\beta-1}} \tag{5.12}$$

and the thermal state is

$$\hat{\rho}_{th} = \sum_{n_1;n_2=0}^{\infty} \frac{\overline{n}^{n_1+n_2}}{(\overline{n}+1)^{n_1+n_2+2}} \left|n_1;n_2\right\rangle \left\langle n_1;n_2\right|. \tag{5.13}$$

This is how thermal states are described by a density operator, and are considered "classical" beams, since they are indistinguishable mixed states, knowing their probability helps to characterize the system [11, 12]. In the following we will make use of a thermal state for a system described by the Hamiltonian of a harmonic oscillator, which will enter on one of the inputs of a BS, which will allow us to study the correlations for each output arm.

5.3 Beam Splitter in a thermal state

Considerer a general beam splitter with two inputs, 1 and 2, whose unitary transformation is described by

$$\hat{U}_{bs}(\zeta) = \exp\left[\zeta \hat{a}_1^\dagger a_2 - \zeta^* \hat{a}_2^\dagger a_1\right]. \tag{5.14}$$

Now if we introduce a thermal state ρ in one of the inputs in the beam splitter and an empty state in the other input, as shown in Figure 5.1, a new thermal state $\hat{\rho}_{th-bs}$ will be obtained

$$\hat{\rho}_{bs} = \hat{U}_{bs}(\zeta)\hat{\rho}_{th}^{\text{input}}\hat{U}_{bs}^\dagger(\zeta), \tag{5.15}$$

the normalized thermal state $\hat{\rho}_{th}^{\text{input}}$ is,

$$\hat{\rho}_{th}^{\text{input}} = \left(1 - \mathrm{e}^{-\hbar\omega\beta}\right) \sum_{n=0}^{\infty} \mathrm{e}^{-n\hbar\omega\beta} \left|0;n\right\rangle_N {}_N\!\left\langle 0;n\right|, \tag{5.16}$$

where the subscripts on the bra and ket denote the base in which we are using, in this case N denoted Fock's basis.

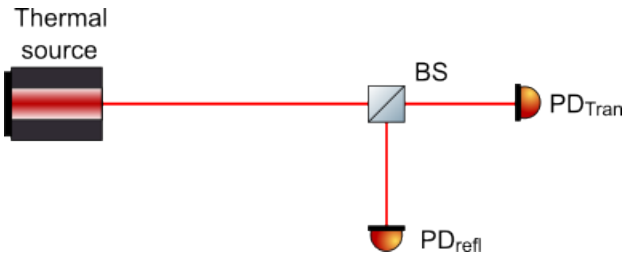

Figure 5.1: Experimental setup where a light is input from a thermal source, and an empty state is input from the other input, resulting in two output beams.

Considering the Schwinger adimensionless relations, with ladder operators in 'Cartesian' coordinates [65],

$$\hat{J}_+ \equiv \hat{a}_1^\dagger \hat{a}_2, \qquad \hat{J}_- \equiv \hat{a}_2^\dagger \hat{a}_1, \tag{5.17}$$

it is possible to write the beam splitter operator in terms of the rising and lowering angular momentum operators

$$\hat{U}_{bs}(\zeta) = \exp\left[\zeta \hat{J}_+ - \zeta^* \hat{J}_-\right], \tag{5.18}$$

so it is convenient to write $\hat{\rho}_{th}^{\text{input}}$ in the base of Schwinger J. We observe that the operators in this representation equation (5.17) are equivalent to those presented in the previous section equation (4.2). Therefore, so we can write

$$j = \frac{n_1 + n_2}{2}, \qquad m = \frac{n_1 - n_2}{2}. \tag{5.19}$$

Considering the scenario where $n_1 = 0$ and $n_2 = n$, where n represents the total number of excitations of the system, we can express the states $\left|0;n\right\rangle_N$ its terms of j and m, as:

$\left\|n_1;n_2\right\rangle_N$	$\left\|j;\,m\right\rangle_J$
$\left\|0;0\right\rangle_N$	$\left\|0;0\right\rangle_J$
$\left\|0;1\right\rangle_N$	$\left\|\frac{1}{2};-\frac{1}{2}\right\rangle_J$
$\left\|0;2\right\rangle_N$	$\left\|1;-1\right\rangle_J$
$\vdots$	$\vdots$

The subscript J in the bras and kets will represent the base of the angular momentum. These relations must satisfy,

$$\hat{J}_{\pm} \left| j; \pm j \right\rangle_J = 0. \tag{5.20}$$

So rewritting equation (5.16)

$$\hat{\rho}_{th}^{\text{input}} = \left(1 - \mathrm{e}^{-\hbar\omega\beta}\right) \sum_{j=0,1/2,1,\ldots} \mathrm{e}^{-2j\hbar\omega\beta} \left| j; -j \right\rangle_J {}_J\!\left\langle j; -j \right|, \tag{5.21}$$

which can be expressed in terms of n but in J bases, this is,

$$\hat{\rho}_{th}^{\text{input}} = \left(1 - \mathrm{e}^{-\hbar\omega\beta}\right) \sum_{n=0}^{\infty} \mathrm{e}^{-n\hbar\omega\beta} \left| \frac{n}{2}; -\frac{n}{2} \right\rangle_J {}_J\!\left\langle \frac{n}{2}; -\frac{n}{2} \right|, \tag{5.22}$$

Now it is enough to act the unitary operator of the BS to the left $\hat{U}_{bs}(\zeta) \left| j; -j \right\rangle_J$, to later obtain its conjugate this is ${}_J\!\left\langle j; -j \right| \hat{U}_{bs}^{\dagger}(\zeta)$.

To achieve this we will follow a series of steps. First using the disentangling relations, we can rewritten eq.(5.18), like

$$\hat{U}_{bs}(\zeta) = \exp\left[\zeta \hat{J}_+ - \zeta^* \hat{J}_-\right] = \exp\left[A_+ \hat{J}_+\right] \exp\left[\ln(A_0) \hat{J}_0\right] \exp\left[A_- \hat{J}_-\right], \tag{5.23}$$

Where A_+, A_-, A_0 are coefficients that can be determined by means of the Masashi-Ban formulas described in [66]. Which indicates that the coefficients for the normal order decomposition are

$$A_+ = \ \mathrm{e}^{-i\phi} \tan(\theta),\ A_- = -\mathrm{e}^{i\phi} \tan(\theta),\ A_0 = \cos^{-2}(\theta), \tag{5.24}$$

so that

$$\hat{U}_{bs}(\theta, \phi) = \exp\left[\mathrm{e}^{-i\phi} \tan(\theta) \hat{J}_+\right] \exp\left[-\ln\big(\cos^2(\theta)\big) \hat{J}_0\right] \exp\left[-\mathrm{e}^{i\phi} \tan(\theta) \hat{J}_-\right]. \tag{5.25}$$

Now we can operate on a state $\left| j, -j \right\rangle_J$,

$$\hat{U}_{bs}(\theta, \phi) \left| j; -j \right\rangle_J = (\cos^2(\theta))^j \exp\left[\mathrm{e}^{-i\phi} \tan(\theta) \hat{J}_+\right] \left| j; -j \right\rangle_J.$$

Let $\kappa = \cos(\theta)$ and $\lambda = \mathrm{e}^{-i\phi} \tan(\theta)$

$$\kappa^{2j} \exp\left[\lambda \hat{J}_+\right] \left| j; -j \right\rangle_J = \kappa^{2j} \sum_{l=0}^{\infty} \frac{(\lambda)^l}{l!} \hat{J}_+ \left| j; -j \right\rangle_J \tag{5.26}$$

$$= \kappa^{2j} \sum_{k=0}^{2j} (\lambda)^k \left[\frac{(2j)!}{(2j-k)!(k)!}\right]^{1/2} \left| j; -j+k \right\rangle_J^{BS}. \tag{5.27}$$

Finally, with $\hat{U}_{bs}(\theta, \phi) \equiv \hat{U}_{bs}$

$$\hat{U}_{bs} \left| j; -j \right\rangle_J = \kappa^{2j} \sum_{k=0}^{2j} (\lambda)^k \binom{2j}{k}^{1/2} \left| j; -j+k \right\rangle_J^{BS}, \tag{5.28}$$

in terms of n,

$$\hat{U}_{bs} \left| \frac{n}{2}; -\frac{n}{2} \right\rangle_J = \kappa^n \sum_{k=0}^{n} (\lambda)^k \binom{n}{k}^{1/2} \left| \frac{n}{2}; -\frac{n}{2}+k \right\rangle_J^{BS}. \tag{5.29}$$

Now we have everything necessary to obtain the thermal state $\hat{\rho}_{tbs}$, defined in (5.15):

$$\begin{aligned}\hat{\rho}_{bs} &= (1-\gamma)\sum_{n=0}^{\infty}\gamma^n\hat{U}_{bs}\left|\frac{n}{2};-\frac{n}{2}\right\rangle_J{}_J\left\langle\frac{n}{2};-\frac{n}{2}\right|\hat{U}_{bs}^{\dagger}\\ &= (1-\gamma)\sum_{n=0}^{\infty}\gamma^n\kappa^{2n}\sum_{k=0}^{n}(\lambda)^k\binom{n}{k}^{1/2}\sum_{l=0}^{n}(\lambda^*)^l\binom{n}{l}^{1/2}\left|\frac{n}{2};-\frac{n}{2}+k\right\rangle_J^{BS\ BS}{}_J\left\langle\frac{n}{2};-\frac{n}{2}+l\right|\\ &= (1-\gamma)\sum_{n=0}^{\infty}\gamma^n\kappa^{2n}\sum_{k=0}^{n,l}(\lambda)^k(\lambda^*)^l\left[\binom{n}{k}\binom{n}{l}\right]^{1/2}\left|\frac{n}{2};-\frac{n}{2}+k\right\rangle_J^{BS\ BS}{}_J\left\langle\frac{n}{2};-\frac{n}{2}+l\right|, \quad (5.30)\end{aligned}$$

where $\gamma = \mathrm{e}^{-\hbar\omega\beta}$. Therefore $\hat{\rho}_{bs}$ given by eq.(5.30) is the output thermal state of the beam splitter. In the Fock basis,

$$\hat{\rho}_{bs} = (1-\gamma)\sum_{n=0}^{\infty}\gamma^n\kappa^{2n}\sum_{k,l=0}^{n}(\lambda)^k(\lambda^*)^l\left[\binom{n}{k}\binom{n}{l}\right]^{1/2}|k;n-k\rangle_N^{BS\ BS}{}_N\langle l;n-l|\,, \quad (5.31)$$

Substituting κ and λ, and

$$\kappa^{2n}\sum_{k,l=0}^{n}(\lambda)^k(\lambda^*)^l = [\cos(\theta)]^{2n}[\tan(\theta)]^{k+l}\,\mathrm{e}^{-ik\phi}\mathrm{e}^{il\phi} = \mu^{k+l}\kappa^{2n-k-l}\nu^{k+l}. \quad (5.32)$$

where $\kappa = \cos(\theta)$, $\mu = \mathrm{e}^{-i\phi}$, $\nu = \sin(\theta)$,

$$\hat{\rho}_{bs} = (1-\gamma)\sum_{n=0}^{\infty}\gamma^n\sum_{k,l=0}^{n}\left[\binom{n}{k}\binom{n}{l}\right]^{1/2}\mu^{k-l}\kappa^{2n-k-l}\nu^{k+l}\,|k;n-k\rangle_N^{BS\ BS}{}_N\langle l;n-l|\,, \quad (5.33)$$

In terms of the mean number of photons, $\overline{n}$ or $\gamma = \mathrm{e}^{-\hbar\omega\beta} = \frac{\overline{n}}{\overline{n}+1}$, we have [12]

$$\hat{\rho}_{bs} = \sum_{n=0}^{\infty}\frac{\overline{n}^n}{(\overline{n}+1)^{n+1}}\sum_{k,l=0}^{n}\left[\binom{n}{k}\binom{n}{l}\right]^{1/2}\mu^{k-l}\kappa^{2n-k-l}\nu^{k+l}\,|k;n-k\rangle_N^{BS\ BS}{}_N\langle l;n-l|\,, \quad (5.34)$$

With this information we now ask ourselves what is the probability of obtaining a certain state at the output of the beam splitter? To answer this we will make use of an arbitrary state $|a,b\rangle_N^{BS}$, so the probability of that state will be,

$$P_{a,b} = {}_N^{BS}\langle a;b|\,\hat{\rho}_{bs}\,|a;b\rangle_N^{BS} \quad (5.35)$$

Then

$$\begin{aligned}P_{a,b} &= (1-\gamma)\sum_{n=0}^{\infty}\gamma^n\sum_{k,l=0}^{n}\left[\binom{n}{k}\binom{n}{l}\right]^{1/2}\mu^{k-l}\kappa^{2n-k-l}\nu^{k+l}\,{}_N^{BS}\langle a,b|\,|k;n-k\rangle_N^{BS\ BS}{}_N\langle l;n-l|a;b\rangle_N^{BS},\\ &= (1-\gamma)\sum_{n=0}^{\infty}\gamma^n\sum_{k,l=0}^{n}\left[\binom{n}{k}\binom{n}{l}\right]^{1/2}\mu^{k-l}\kappa^{2n-k-l}\nu^{k+l}\delta_{a,k}\delta_{b,n-k}\delta_{a,l}\delta_{b,n-l}\\ &= (1-\gamma)\gamma^{a+b}\binom{a+b}{a}\kappa^{2b}\nu^{2a} \quad (5.36)\end{aligned}$$

Replacing the terms

$$P_{a,b} = \frac{\overline{n}^{a+b}}{(\overline{n}+1)^{a+b+1}}\binom{a+b}{a}[\cos\theta]^{2b}[\sin\theta]^{2a}\,. \quad (5.37)$$

Figure 5.2 shows the probability distribution for a 50 : 50 symmetric beam splitter making use of (5.37), as well as the experimental probability, in both cases with $\overline{n} \approx 6$ and $\theta = \pi/4$.

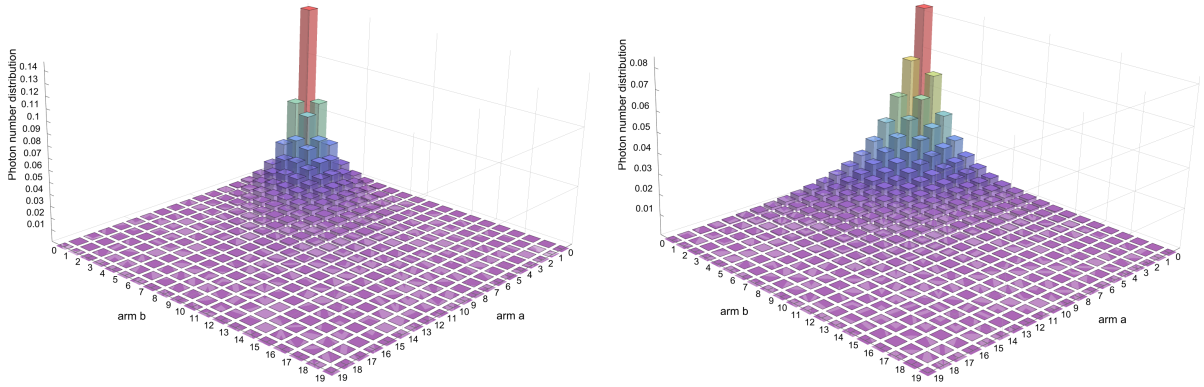

Figure 5.2: Theoretical probability distribution (left) and experimental probability distribution (right) for a $50:50$ symmetric beam splitter.

By fitting the experimental data with the theoretical data, we find that the experimental system behaves best as the one corresponding to a $35:65$ beam splitter, as shown in Figure 5.3.

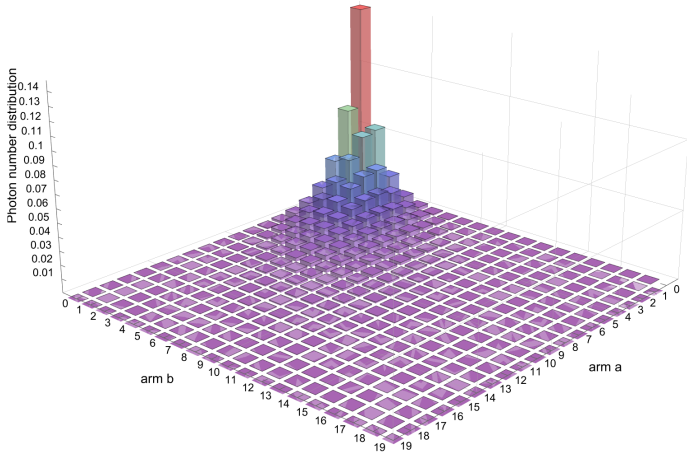

Figure 5.3: Theoretical probability distribution for a $35:65$ symmetric beam splitter.

Given the information provided by other experimental systems of thermal sources [67], the discrepancies observed between the theoretical and experimental data can be attributed to fluctuations, since the grouping effect presented by thermal light increases the probability that the fluctuations exceed the expected average in the number of photons measured in the detectors.

Chapter 6

Conclusions and perspectives

In this work, from an isotropic harmonic oscillator Hamiltonian in two dimensions, we have obtained Hermite-Gauss and Laguerre-Gauss states.

The Hermite-Gauss states are described by transverse excitation numbers and describe the modes of beams that have a square structure, called Hermite-Gauss modes. The intensity distribution shows radial dispersion. Compared to with the fundamental mode, the mean value of the transverse excitation numbers is associated with the number of modes in the corresponding direction.

The Laguerre-Gauss modes are described by the radial and azimuthal numbers and describe the modes of beams with radial structure. The intensity distribution is constructed using rings, where the number of rings is related to the radial number and the width of the rings is defined by the azimuthal number.

With these results, we use the known Gilmore-Perelomov and Barut-Girardelo coherent states in terms of the radial and azimuthal number. First for the $SU(1,1)$ group representation, we find that it is possible to define new coherent states that have a relation with a Bargmann parameter defined in terms of the azimuthal number. This establishes that there are two subspaces with the same Bargmann parameter. In addition, the probability density has a similar structure to the intensity distribution of the Laguerre-Gauss modes. In the phase structure, the azimuthal number is directly proportional to the number of vortices.

For the coherent states in the $SU(2)$ representation, only Gilmore-Perelomov states are found. The spin quantum number j described in terms of the radial and azimuthal numbers can be regarded as equivalent to the Bargann parameter. The phase transitions are proportional to the value of the spin number. The probability density are similar to the intensity distribution of the Hermite-Gauss modes, this implies that the phase structure does not contain any vortices.

In addition to coherent states, for those systems that need a study that takes into account their statistical behavior, there are mixed states. Considered here are the thermal states, which can be written in terms of the Boltzmann constant or the average of photons, which have been discussed from the representations of $SU(1,1)$ and $SU(2)$. For the case of $SU(1,1)$ group generators, we can obtain the thermal states, which are written as the sum of the density operator for $\ell \geq 0$ with the density operator corresponding to $\ell < 0$.

The $SU(2)$ thermal states allow to study theoretically in an efficient way the behavior of introducing a thermal state and a vacuum state into the corresponding inputs of beam splitter, resulting in a new output thermal state. However, when studying the correlations, it is ideal to write the output thermal state in the Fock basis to study the number of excitations of the system. This also provides a simple way to compare the theoretical and experimental data. An analysis of the results shows a discrepancy between the theoretical and experimental data. This can be produced by different factors, such as the sensitivity of the sensors. The fluctuations and the nature of the thermal light, that in the experiment increase the reading for the number of photons, giving an opportunity to extend the theoretical model developed here.

In conclusion, the coherent states presented here are interesting due to their behavior and the versatility of their parameters to explain the system. The work presented is not complete and we are currently still expanding and developing the topic presented here, together with theoretical and experimental researchers from several universities. It is hoped that this analysis will provide the framework for future studies and allow us to go beyond coherent states and create a more complete analysis of thermal states. And this since here the thermal states have been studied only from the perspective of their number of excitations, leaving the opportunity to explore them considering the radial and azimuthal numbers. The analysis of their possible entanglement and experimental comparison could help advance the development of novel aspects of quantum information, such as the creation of protocols in quantum key distribution and in the preparation of distant states.

Bibliography

[1] E. National Academies of Sciences and Medicine, *Quantum Computing: Progress and Prospects*. Washington, DC: The National Academies Press, 2019.

[2] P. Goldner, A. Ferrier, and O. Guillot-Noël, "Chapter 267 - rare earth-doped crystals for quantum information processing," vol. 46 of *Handbook on the Physics and Chemistry of Rare Earths*, pp. 1–78, Elsevier, 2015.

[3] M. A. Nielsen and I. L. Chuang, *Quantum Computation and Quantum Information: 10th Anniversary Edition*. Cambridge University Press, 2010.

[4] T. D. Ladd, F. Jelezko, R. Laflamme, Y. Nakamura, C. Monroe, and J. L. O'Brien, "Quantum computers," *Nature*, vol. 464, pp. 45–53, Mar 2010.

[5] K. Wagner, J. Janousek, V. Delaubert, H. Zou, C. Harb, N. Treps, J. F. Morizur, P. K. Lam, and H. A. Bachor, "Entangling the spatial properties of laser beams," *Science*, vol. 321, no. 5888, pp. 541–543, 2008.

[6] D. Browne, S. Bose, F. Mintert, and M. Kim, "From quantum optics to quantum technologies," *Progress in Quantum Electronics*, vol. 54, pp. 2–18, 2017. Special issue in honor of the 70th birthday of Professor Sir Peter Knight FRS.

[7] L. Jun, *Physical Realization of Harmonic Oscillator Quantum Computer*, pp. 29–34. Berlin, Heidelberg: Springer Berlin Heidelberg, 2012.

[8] S. D. Bartlett, H. de Guise, and B. C. Sanders, "Quantum encodings in spin systems and harmonic oscillators," *Phys. Rev. A*, vol. 65, p. 052316, May 2002.

[9] G. Nienhuis, "Chapter 5 - operators in paraxial quantum optics," in *Structured Light for Optical Communication* (M. D. Al-Amri, D. L. Andrews, and M. Babiker, eds.), Nanophotonics, pp. 107–137, Elsevier, 2021.

[10] P. Meystre and M. Sargent, *Field Quantization*, pp. 299–325. Berlin, Heidelberg: Springer Berlin Heidelberg, 2007.

[11] R. Loudon, *The Quantum Theory of Light*. Oxford: Clarendon Press, third ed., 2000.

[12] C. Gerry and P. Knight, *Introductory Quantum Optics*. Cambridge University Press, 2004.

[13] L. de la Peña, *Introducción a la mecánica cuántica*. Ediciones Científicas Universitarias, Fondo de Cultura Economica, 2014.

[14] L. Mandel and E. Wolf, *Optical coherence and quantum optics*. Cambridge university press, 1995.

[15] J. Cortés-Tamayo, "Estados coherentes del campo de radiación," *Revista Mexicana de Física*, vol. 38, no. 2, pp. 309–331, 1991.

[16] M. R. Kibler and M. Daoud, "Generalized coherent states for polynomial weyl-heisenberg algebras," *arXiv preprint arXiv:1201.1811*, 2012.

[17] A. El Kinani and M. Daoud, "Generalized intelligent states for an arbitrary quantum system," *Journal of Physics A: Mathematical and General*, vol. 34, no. 26, p. 5373, 2001.

[18] S. Lyagushyn and A. Sokolovsky, "Description of field states with correlation functions and measurements in quantum optics," in *Quantum Optics and Laser Experiments* (S. Lyagushyn, ed.), ch. 1, Rijeka: IntechOpen, 2012.

[19] A. E. Willner et al., "Optical communications using orbital angular momentum beams," *Adv. Opt. Photon.*, vol. 7, pp. 66–106, Mar 2015.

[20] A. M. Yao and M. J. Padgett, "Orbital angular momentum: origins, behavior and applications," *Adv. Opt. Photon.*, vol. 3, pp. 161–204, Jun 2011.

[21] L. Allen, M. W. Beijersbergen, R. J. C. Spreeuw, and J. P. Woerdman, "Orbital angular momentum of light and the transformation of laguerre-gaussian laser modes," *Phys. Rev. A*, vol. 45, pp. 8185–8189, Jun 1992.

[22] I. Bialynicki-Birula and Z. Bialynicka-Birula, "Beams of electromagnetic radiation carrying angular momentum: The riemann–silberstein vector and the classical–quantum correspondence," *Optics Communications*, vol. 264, no. 2, pp. 342–351, 2006. Quantum Control of Light and Matter.

[23] M. Babiker, V. Lembessis, K. Köksal, and J. Yuan, "Chapter 2 - structured light," in *Structured Light for Optical Communication* (M. D. Al-Amri, D. L. Andrews, and M. Babiker, eds.), Nanophotonics, pp. 37–76, Elsevier, 2021.

[24] M. Krenn, M. Malik, M. Erhard, and A. Zeilinger, "Orbital angular momentum of photons and the entanglement of laguerre-gaussian modes," *Philosophical Transactions of The Royal Society A Mathematical Physical and Engineering Sciences*, vol. 375, 02 2017.

[25] Y. Shen, X. Wang, Z. Xie, C. Min, X. Fu, Q. Liu, M. Gong, and X. Yuan, "Optical vortices 30 years on: Oam manipulation from topological charge to multiple singularities," *Light: Science & Applications*, vol. 8, p. 90, 10 2019.

[26] O. S. Magaña-Loaiza and R. W. Boyd, "Quantum imaging and information," *Reports on Progress in Physics*, vol. 82, p. 124401, nov 2019.

[27] L. Chen, "Quantum discord of thermal two-photon orbital angular momentum state: mimicking teleportation to transmit an image," *Light: Science & Applications*, vol. 10, p. 148, 07 2021.

[28] B. Sephton et al., "Stimulated teleportation of high-dimensional information with a nonlinear spatial mode detector," 2022.

[29] X.-M. Hu, Y. Guo, B.-H. Liu, C.-F. Li, and G.-C. Guo, "Progress in quantum teleportation," *Nature Reviews Physics*, vol. 5, pp. 339–353, Jun 2023.

[30] T. J. Sturges et al., "Quantum simulations with multiphoton fock states," *npj Quantum Information*, vol. 7, p. 91, Jun 2021.

[31] K. Fujii, "Introduction to coherent states and quantum information theory," 2002.

[32] A. Walton, A. Ghesquiere, G. Brumpton, D. Jennings, and B. Varcoe, "Thermal state quantum key distribution," *Journal of Physics B: Atomic, Molecular and Optical Physics*, vol. 54, p. 185501, oct 2021.

[33] K.-D. Wu, T. Theurer, G.-Y. Xiang, C.-F. Li, G.-C. Guo, M. Plenio, and A. Streltsov, "Quantum coherence and state conversion: theory and experiment," *npj Quantum Information*, vol. 6, 12 2020.

[34] X. Wang, B. C. Sanders, and S. hua Pan, "Entangled coherent states for systems with su(2) and su(1,1) symmetries," *Journal of Physics A: Mathematical and General*, vol. 33, p. 7451, oct 2000.

[35] M. Zhan, F. Jia, J. Huang, H. Zhang, and L. Hu, "Representation of the coherent state for a beam splitter operator and its applications," *Communications in Theoretical Physics*, vol. 74, p. 035101, feb 2022.

[36] M. S. Kim, W. Son, V. Bužek, and P. L. Knight, "Entanglement by a beam splitter: Nonclassicality as a prerequisite for entanglement," *Phys. Rev. A*, vol. 65, p. 032323, Feb 2002.

[37] C. Brif, A. Vourdas, and A. Mann, "Analytic representations based on su (1 , 1) coherent states and their applications," *Journal of Physics A: Mathematical and General*, vol. 29, p. 5873, sep 1996.

[38] M. Novaes, "Some basics of su(1,1)," *Revista Brasileira de Ensino de Física*, vol. 26, no. 4, pp. 351 – 357, 2004.

[39] R. M. de Araújo et al., "Experimental study of quantum thermodynamics using optical vortices," *Journal of Physics Communications*, vol. 2, p. 035012, mar 2018.

[40] H. Kogelnik and T. Li, "Laser beams and resonators," *Appl. Opt.*, vol. 5, pp. 1550–1567, Oct 1966.

[41] G. Nienhuis, *Ray optics, wave optics and quantum mechanics*, p. 98–134. Cambridge University Press, 2012.

[42] N. Zettili, *Quantum Mechanics: Concepts and Applications*. Wiley, 2009.

[43] C. Cohen-Tannoudji, B. Diu, F. Laloë, S. Hemley, N. Ostrowsky, and D. Ostrowsky, *Quantum Mechanics*. No. v. 1 in A Wiley - Interscience publication, Wiley, 1977.

[44] E. G. Abramochkin and V. G. Volostnikov, "Generalized gaussian beams," *Journal of Optics A: Pure and Applied Optics*, vol. 6, p. S157, apr 2004.

[45] J.-M. Liu, *Photonic Devices*. Cambridge University Press, 2005.

[46] E. Karimi et al., "Radial quantum number of laguerre-gauss modes," *Physical Review A*, vol. 89, p. 062813, 06 2014.

[47] I. Kimel and L. Elias, "Relations between hermite and laguerre gaussian modes," *IEEE Journal of Quantum Electronics*, vol. 29, no. 9, pp. 2562–2567, 1993.

[48] W. N. Plick and M. Krenn, "Physical meaning of the radial index of laguerre-gauss beams," *Phys. Rev. A*, vol. 92, p. 063841, Dec 2015.

[49] L. Lugiato, F. Prati, and M. Brambilla, *Nonlinear Optical Systems*. Cambridge University Press, 2015.

[50] K. Blum, *Density matrix theory and applications; 3rd ed.* Springer series on atomic, optical, and plasma physics, Berlin: Springer, 2012.

[51] P. W. Atkins and J. C. Dobson, "Angular momentum coherent states," *Proceedings of the Royal Society of London. Series A, Mathematical and Physical Sciences*, vol. 321, no. 1546, pp. 321–340, 1971.

[52] D. Bhaumik, T. Nag, and B. Dutta-Roy, "Coherent states for angular momentum," *Journal of Physics A: Mathematical and General*, vol. 8, p. 1868, dec 1975.

[53] C. C. Gerry, "Correlated two-mode su (1, 1) coherent states: nonclassical properties," *JOSA B*, vol. 8, no. 3, pp. 685–690, 1991.

[54] A. O. Barut and L. Girardello, "New "Coherent" States associated with non-compact groups," *Communications in Mathematical Physics*, vol. 21, pp. 41–55, Mar. 1971.

[55] R. F. Bishop and A. Vourdas, "Coherent mixed states and a generalised p representation," *Journal of Physics A: Mathematical and General*, vol. 20, p. 3743, aug 1987.

[56] J. J. Sakurai and J. Napolitano, *Modern Quantum Mechanics*. Cambridge University Press, 2 ed., 2017.

[57] A. M. Perelomov, "Generalized coherent states and some of their applications," *Soviet Physics Uspekhi*, vol. 20, p. 703, sep 1977.

[58] K. Wodkiewicz and J. H. Eberly, "Coherent states, squeezed fluctuations, and the su(2) am su(1,1) groups in quantum-optics applications," *J. Opt. Soc. Am. B*, vol. 2, pp. 458–466, Mar 1985.

[59] D. Ojeda-Guillén, R. Mota, and V. Granados, "Spin number coherent states and the problem of two coupled oscillators*," *Communications in Theoretical Physics*, vol. 64, p. 34, jul 2015.

[60] Y. Shen, "Rays, waves, su(2) symmetry and geometry: toolkits for structured light," *Journal of Optics*, vol. 23, p. 124004, nov 2021.

[61] J. Pan, H. Wang, Z. Shi, Y. Shen, X. Fu, and Q. Liu, "Frequency-astigmatism asymmetric nonlinear conversion of structured light lasers," 2023.

[62] E. Díaz-Bautista, J. Negro, and L. Nieto, "Coherent states in the symmetric gauge for graphene under a constant perpendicular magnetic field," *The European Physical Journal Plus*, vol. 136, 05 2021.

[63] Z. Gress and S. C. y Cruz, *Hermite Coherent States for Quadratic Refractive Index Optical Media*, pp. 323–339. Cham: Springer International Publishing, 2019.

[64] D. S. Simon, G. Jaeger, and A. V. Sergienko, *Ghost Imaging and Related Topics*, pp. 131–158. Cham: Springer International Publishing, 2017.

[65] R. Campos, B. Saleh, and M. Teich, "Quantum-mechanical lossless beam splitter: Su(2) symmetry and photon statistics," *Physical Review A*, vol. 40, pp. 1371–1384, 09 1989.

[66] M. Ban, "Decomposition formulas for su(1, 1) and su(2) lie algebras and their applications in quantum optics," *J. Opt. Soc. Am. B*, vol. 10, pp. 1347–1359, Aug 1993.

[67] G. L. Zanin et al., "Experimental quantum thermodynamics with linear optics," *Brazilian Journal of Physics*, vol. 49, pp. 783–798, 2019.